ARMY RESEARCH LABORATORY

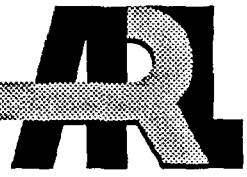

Thermocouples for Interior Ballistic Temperature Measurements

Stephen L. Howard
Lang-Mann Chang
Douglas E. Kooker

ARL-MR-146 August 1994

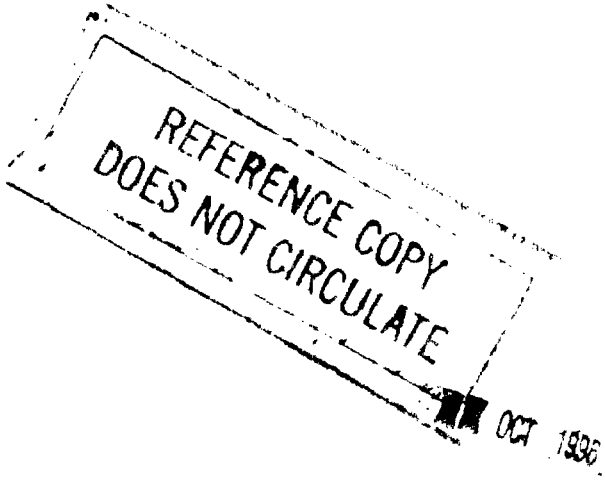

NOTICES

Destroy this report when it is no longer needed. DO NOT return it to the originator.

Additional copies of this report may be obtained from the National Technical Information Service, U.S. Department of Commerce, 5285 Port Royal Road, Springfield, VA 22161.

The findings of this report are not to be construed as an official Department of the Army position, unless so designated by other authorized documents.

The use of trade names or manufacturers' names in this report does not constitute indorsement of any commercial product.

REPORT DOCUMENTATION PAGE

Form Approved
OMB No. 0704-0188

1. AGENCY USE ONLY *(Leave blank)*	2. REPORT DATE	3. REPORT TYPE AND DATES COVERED
	August 1994	Final, Oct 1991 - Sept 1993

4. TITLE AND SUBTITLE

Thermocouples for Interior Ballistic Temperature Measurements

5. FUNDING NUMBERS

PR: #1L161102AH43

6. AUTHOR(S)

Stephen L. Howard, Lang-Mann Chang, and Douglas E. Kooker

7. PERFORMING ORGANIZATION NAME(S) AND ADDRESS(ES)

U.S. Army Research Laboratory
ATTN: AMSRL-WT-PA
Aberdeen Proving Ground, MD 21005-5066

8. PERFORMING ORGANIZATION REPORT NUMBER

9. SPONSORING/MONITORING AGENCY NAMES(S) AND ADDRESS(ES)

U.S. Army Research Laboratory
ATTN: AMSRL-OP-AP-L
Aberdeen Proving Ground, MD 21005-5066

10.SPONSORING/MONITORING AGENCY REPORT NUMBER

ARL-MR-146

11. SUPPLEMENTARY NOTES

12a. *DISTRIBUTION/AVAILABILITY STATEMENT*

Approved for public release; distribution unlimited.

12b. DISTRIBUTION CODE

13. ABSTRACT *(Maximum 200 words)*

Flamespreading processes during the ignition of ballistic events have long been studied by pressure measurements and visual records from high-speed film. While optical temperature measurements have been utilized, they are not useful much below 1500 K. This report describes a fine-wire thermocouple probe designed to measure gas temperature in a propellant bed over the range from the initial propellant bed temperature to over 2000 K. Several diameters of thermocouple wire are tested for survivability and time response in the simulated pressure-wave environment of ignition of a propellant bed. Examples of temperature histories during ignition of M30A1 and M43 propellants are also included.

14. SUBJECT TERMS

Ignition Studies; Temperature;Primers; Flamespreading; Gun Simulator

15. NUMBER OF PAGES

48

16. PRICE CODE

17. SECURITY CLASSIFICATION OF REPORT	18. SECURITY CLASSIFICATION OF THIS PAGE	19. SECURITY CLASSIFICATION OF ABSTRACT	20. LIMITATION OF ABSTRACT
UNCLASSIFIED	UNCLASSIFIED	UNCLASSIFIED	UL

INTENTIONALLY LEFT BLANK.

ACKNOWLEDGMENTS

The authors wish to thank Messrs. T. Rosenberger and M. Ridgley at the Indoor Range Facility of the U. S. Army Research Laboratory (ARL) for their assistance in performing the test firings. The authors would also like to thank H. A. McElroy of the Olin Ordnance Corporation who, under provisions of an ARL-Olin unfunded study agreement, supplied the ball powder propellant used in the igniter chamber.

INTENTIONALLY LEFT BLANK.

TABLE OF CONTENTS

INTENTIONALLY LEFT BLANK.

LIST OF FIGURES

INTENTIONALLY LEFT BLANK.

LIST OF TABLES

INTENTIONALLY LEFT BLANK.

1. INTRODUCTION

Crucial to the gun interior ballistic cycle is the propagation of an ignition front or "flame zone" through the bed of unburned propellant grains or sticks. If this process is rapid and reproducible, few concerns are promulgated. However, if ignition of a particular propellant is difficult (such as that designed for low-vulnerability, or LOVA, propellants), and if the ignition system is not sufficient in its operation, significant delay to ignition can transform an otherwise smooth flamespreading process into a process that can promote large amplitude pressure waves in a combustion chamber (Horst 1983, 1986; Chang, Deas, and Grosh 1991). Pressure waves have been implicated in previous catastrophic overpressures of several artillery and tank cannons (May and Horst 1978; Horst 1986) and further study of their causes is needed.

Almost without exception, the ignition process in gun systems is dominated by a three-dimensional flow. As a consequence, it is difficult to isolate and investigate the physics of the flamespreading event. A current investigation (Kooker, Howard, and Chang 1993; Kooker, Chang, and Howard 1993) attempts to reduce the three-dimensional event to a one-dimensional planar wave that propagates through a bed of granular propellant. It is hoped that this physical simulation will replicate and allow elucidation of the pressure and thermal environments present in typical gun chambers. While this investigation is primarily aimed at obtaining information that will ultimately improve the ignition systems for gun systems that utilize LOVA propellants, the focus of this report describes the sensors designed to monitor the thermal environment in the gas phase during the flamespreading event within a propellant bed - such an environment is of great importance to the smooth ignition of all propellants.

Temperature measurements of a combustion event have typically been made utilizing one of two methods - thermocouple or photodetection. Photodetection typically requires detection of light at two or more frequencies emitted from material (gases, liquids, or solids) in the region of interest. Unless information about the spectral emissivity of the mixture is present, it is assumed to be a blackbody emitter (or particles in the gas flow are small enough and in sufficient abundance to be considered an adequate emitter) and the temperature deduced from the intensity ratio of the light frequencies detected (Tourin 1966;

Penzias 1974; Kracek and Benedict 1944; Klingenberg and Mach 1976; McClure 1984). However, inherent in the method is the fact that the measurement is a line-of-sight measurement. In other words, if intervening material that is optically thick (such as combustion gases) is present between the detector and the region of interest, the detector may be pointed at the region of interest but will only record the light emitted within a thin layer (typically quoted as on the order of a few millimeters or less) next to the window that collects the emitted radiation (Kracek and Benedict 1943; Klingenberg and Mach 1976). This gas layer of necessity contains boundary layers that eventually contact the probe and are cooled to some extent. The thickness of the boundary layers and the amount of heat transferred across them are dependent upon many variables. However, the method does have the advantage that mechanical devices are not required to be inserted into the gas flow (intimate contact by such devices with the gas flow changes flow patterns and thermal distributions thereby introducing distortions in the temperature measurement). Another drawback of this technique is that the emitting sample must radiate sufficient light at the selected frequencies. Since typical measurements utilize light frequencies near the visible region, this limitation typically precludes temperature assignment below 1000 K. It is only near or above this temperature that typical materials begin to acquire sufficient energy from the thermal environment to excite sufficient electronic transitions that emit the required frequency of light.

Thermocouple measurements can be subdivided into two categories - heat flux and junction temperature measurements. While a junction similar to one used for junction temperature measurements forms the active area for a heat flux probe, a large difference exists between the two devices. Heat flux measurements often use thin films of metal (typically sputtered onto a substrate with a thickness on the order of 1 μm) to form a junction (the junction is defined as the volume in which two dissimilar metals are brought into intimate contact with each other, typically including a region in which each material diffuses into the other) on a substrate that, for the duration of the experiment, maintains a constant temperature. Since the junction for heat flux measurements is on a substrate that remains at or near a constant temperature that was present prior to the experiment (the assumption of a semi-infinite thermal reservoir that does not change its temperature), the temperature of the junction does not change. Instead, the thermal flux into the substrate induces a voltage in the metals forming the junction. This voltage is proportional to the flux.

On the other hand, the entire junction region of a junction temperature measurement device (hereafter referred to simply as a thermocouple) is fully immersed in the thermal environment. Heat from the junction in the thermal environment to be measured flows through the wires connected to this junction to a second exact junction that is held at a known reference temperature. The heat flow is *not* maintained by the usual Fourier heat conduction effect, but rather, by the electrical Seebeck and Peltier effects. The voltage induced in the wires by the heat flow is proportional to the temperature difference between the two junctions.

Like the photodetection method, the heat flux sensor does not obtain the *local* gas temperature. Rather, it is sensitive to the thermal and gas flows across the sensor that attempt to change its surface temperature. However, this sensor is robust and can be made to survive the entire interior ballistic cycle of a gun. Some sensors of this type also are constructed of a thin constantan wire spot welded to the steel wall of a gun tube. The gun steel/constantan thermocouple junction thus formed is then used to obtain the heat flux into the gun tube (Brosseau and Ward 1976, 1978; Stobie, Brosseau, and Kaste 1980; Brosseau, Stobie, Ward, and Greene 1982).

Thin-wire sensors, on the other hand, can measure the local gas temperature because the thermocouple junction is placed directly in the gas flow. Two main disadvantages, however, are present. One occurs as the junction diameter is reduced in order to decrease the response time. As the wire diameter (and subsequent junction diameter) decreases, the total force imparted by the flowing gases upon the wire can break the wire and interrupt the measurement during the ballistic event. Care must also be taken such that the probe does not greatly affect the flow parameters of the gas flow into which it is placed. The larger the diameter of the thermocouple, the greater are the perturbations to the gas flow; therefore, a compromise between these constraints must be met.

The scope of this report is to relate the design and testing of thin-wire thermocouple sensors that can survive the ignition phase of the ballistic cycle. The ignition phase of the ballistic cycle is simulated in a flow chamber containing granular propellant. Results from both inert and live propellents will be demonstrated.

2. EXPERIMENTAL

2.1 Flamespread Chamber. The flamespread chamber simulator has been described elsewhere (Kooker, Chang, and Howard 1993) and only its important features are discussed here. The simulator chamber consists of an acrylic or aluminum tube machined to fit the inside diameter of an outer steel casing (see Figure 1). The tube has three 12.5-mm-diameter holes with a separation of 50.8 mm along the longitudinal axis. Kistler pressure gauges (Model 211B1) are placed into adapters that fit into these holes and are secured by the outer steel casing. Since it is desired that temperature and pressure are measured concurrently, the thermocouples are placed at the same position along the longitudinal axis as the pressure gauges.

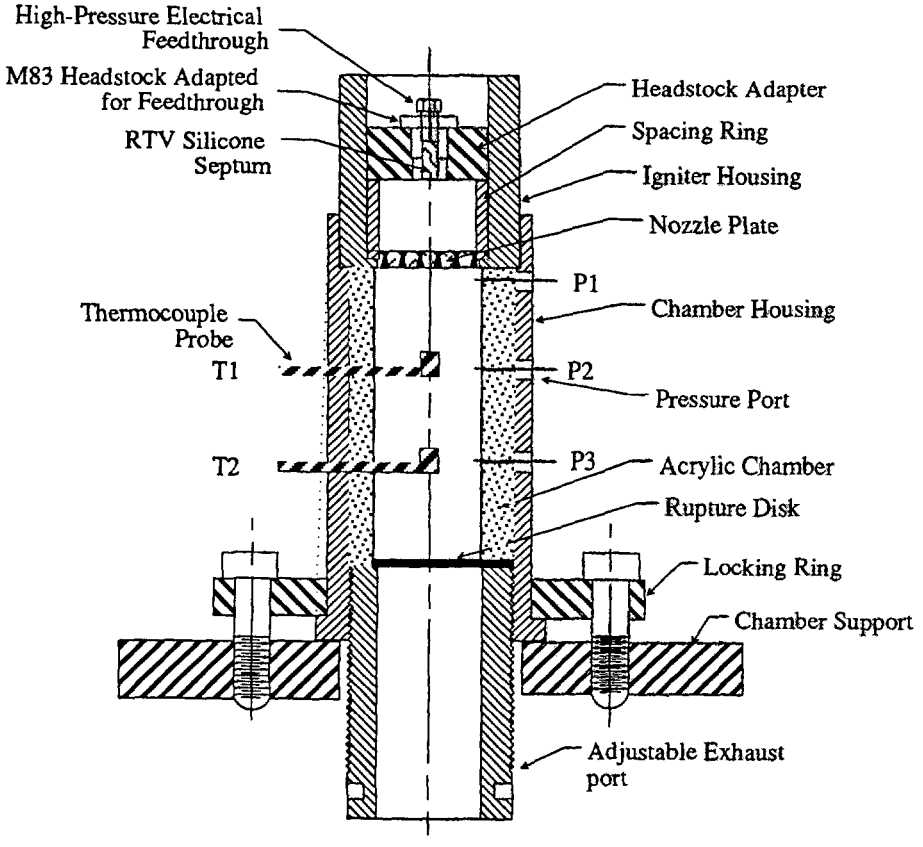

Figure 1. Cross-sectional view of flamespread simulator.

Note: Usage of manufacturer name or model does not constitute endorsement of the product by the U. S. Government or its affiliates.

Only two of the three pressure gauges are located completely within the propellant bed. The first gauge is located at the top of the propellant bed and is partially immersed in the propellant bed. It is used as an indicator of when the igniter chamber diaphragm ruptures and the beginning of the pressure wave through the propellant bed section of the simulator occurs.

In order that the probes did not interfere with each other in the gas flow field, the pressure and temperature probes were mounted to the tube wall nearly opposite (approximately 120°) from each other (see Figure 2). Thermocouple probes of different lengths for different bed penetration depths were fabricated. The object of the different bed penetration depths was to obtain a radial profile within the bed. This profile would be indicative of the degree to which the wave progressing through the bed is planar (the more flat the profile, the more planar the wave). However, for these experiments, only those that placed the thermocouple near the central axis of the simulator tube were utilized.

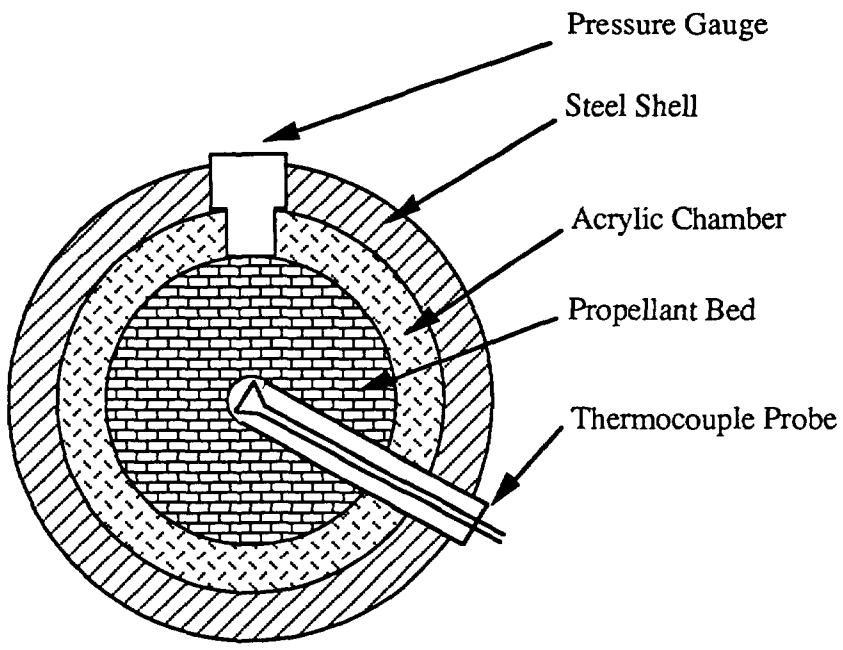

Figure 2. Cross-sectional view of flamespread chamber with pressure and thermocouple probes showing radial placement.

Thermocouples used for this experiment were obtained from Omega Engineering, Inc. Type S (platinum alloyed with 10% rhodium [positive polarity] vs platinum [negative polarity]) bare wire thermocouples were obtained in 3-mil (76 μm), 2-mil (51 μm), and 1-mil (25 μm) wire diameters. The junction was of the beaded variety and was fabricated by the company (the junction diameter, d, was approximately twice the diameter of the wire). Type S thermocouples were chosen for several reasons. Firstly, they are rated for high static temperatures (over 2000 K) and have a fairly linear voltage response with temperature over the range of temperatures to be investigated. The thermocouple material is also resistant to oxidation by certain gas products formed in the combustion of the igniter material and the propellants.

Prior to the experiment, it was not known which diameter wire would provide an adequate time response while surviving the pressure wave traversing the flow chamber. An important part of the experiment was to determine the smallest diameter thermocouple wire that would survive passage of the wave through the propellant bed. Therefore, temperature histories of the three diameters were compared in an effort to ascertain the temperature sensitivities and survivability as a function of time during the short-lived (less than a second) transient that was created in the simulator.

Voltages generated at the thermocouple junction were referenced to 273 K by an electronic ice point obtained from Omega Engineering, Inc. The voltages were then amplified by a Newport Model 70A Diffamp differential amplifier and recorded in both analog and digital modes by the recording equipment in the Indoor Range Facility located in Building 390 of the U. S. Army Research Laboratory (ARL). Pressures were also recorded but will not be discussed in this report (see Kooker, Howard, and Chang 1993).

2.2 Thermocouple Mounts. Since the fine-wire thermocouples selected for use in the simulator do not have the strength to remain in one position (they could be destroyed by grain movement and/or grain contact or they could be pushed away from the initial known position by forces imparted by the gas flow) during the passing of the pressure wave in the flow chamber, a probe mount was designed to hold the junction at a fixed position and yet minimally impede the gas flow about the thermocouple junction.

2.2.1 Original Concept. As shown in Figure 3, the original concept for a thermocouple probe provided for a rigid mount that would attach through the tube wall and extend into the propellant bed perpendicular to the gas flow. At the probe end, the mount had a tubular passage mounted parallel to the gas flow. This passage was smaller than the propellant grains so that propellant grains would not be allowed to enter the passage during propellant bed movement and shear the thermocouple wires. Inside the passage the thermocouple wires would be attached to the interior walls with tape or glue, thereby allowing the junction to be placed in the center of the passage with minimal gas flow restriction.

TOP VIEW (Thermocouple Enlarged for Clarity)

ENLARGED PART - SECTION A-A

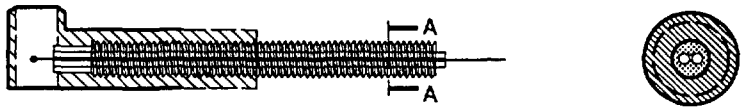

SIDE VIEW

1 cm

Figure 3. Cross-sectional view of original thermocouple mount.

An estimate of the force generated on the probe led to minimum outer diameter of 7.9 mm for a probe stem constructed of mild-carbon steel. However, the probe outer diameter needed to be minimized in order to limit perturbations in the gas flow. On the other hand, the passage needed to be large enough in diameter that gases in the boundary layer cooled by heat transfer to the mount itself would not approach the thermocouple junction and be detected. Only unperturbed gases in the free stream can be present near the junction for accurate measurements. Therefore, this diameter can be as small as the probe

stem if the depth of the flow-imposed boundary layer does not approach the thermocouple junction.

Two different flow regimes must be considered when estimating the boundary layer. At low flow velocities, the flow regime exhibits laminar flow within the probe. At higher flow velocities, turbulent flow begins to form until the transition flow becomes fully turbulent flow. The data in Table 1 for determining the boundary layer thickness were provided directly, or indirectly, by experiments (Kooker, Chang, and Howard 1993), or when stated, as limiting estimates. Experimental conditions were at the thermocouple stations.

Table 1: Data for Boundary Layer Calculations

	Gas Velocity[†] (meter/second)	Viscosity (centipoise)	Temperature (Kelvin)	Pressure (MPa)	Molecular Weight (gram/mole)
Lower limit	40				
Upper limit	300[ξ]				
Experimental	175	0.14[¥]	1200	3.0	25.0[§]

[†]Upper and lower limits are estimates.

[ξ]Obtained from gun simulator results (see Chang and Rocchio 1988).

[§]Obtained from NASA-Lewis calculations (see Gordon and McBride 1976).

[¥]Estimate obtained from experimental conditions (see Liley and Gambill 1973).

At sufficiently high gas velocities, the boundary layer condition can be modelled to first order as flow along a flat plate. If the leading edge of the plate is angled like a knife edge, with the edge angled away from the passage region, a clean separation of the upstream flowlines occurs and the boundary layer will develop from the leading edge. The free-stream gas velocity will also be undisturbed at the entrance of the passage. If the plate Reynolds number (Re_x is characteristic of the ratio of the inertial forces to the viscous forces acting upon the gas flow) is calculated using the formula

$$Re_x = \frac{\rho v x}{\mu} \quad , \qquad (1)$$

where x is the distance from the leading edge along the plate traversed by the gas flow, ρ is the gas density, v is the gas velocity and μ is the viscosity of the gas, then a decision can be

made as to whether the flow is laminar or turbulent. If Re_x is less than approximately 4×10^5 (see Schlichting 1960a), the flow can be considered to be laminar. If Re_x is approximately 4 to 5×10^5, the flow is in transition between laminar and turbulent. At values greatly in excess of 5×10^5, the flow is fully turbulent.

Once the value of Re_x is known, the boundary layer thickness as a function of distance can be calculated. For laminar conditions (Schlichting 1960a), the boundary layer thickness is obtained from Equation 2,

$$\frac{\delta(x)}{x} = 5\left(Re_x\right)^{-1/2} \qquad (2)$$

For turbulent conditions, it is obtained from Equation 3 assuming turbulent flow with a one-seventh order power law for the velocity distribution (Schlichting 1960b),

$$\delta(x) = 0.370x\left(Re_x\right)^{-1/5} \qquad (3)$$

where $\delta(x)$ is the boundary layer thickness as a function of distance x.

Assuming the parameters in Table 1 and a gas density obtained from the ideal-gas law, an estimate of the boundary layer thickness for the smallest length passage (diameter of the probe stem plus sufficient for the knife edge) was obtained. These conditions are listed in Table 2. In all cases, the estimated boundary layer thickness is much less than the radius of the flow passage and, thus, the temperature measurement from the thermocouple represents the gas temperature in the free stream in the propellant bed.

Table 2: Calculated Reynolds Numbers

Condition	Re_x	Boundary Layer Thickness (mm)
Lower velocity limit	410,000	0.06
Upper velocity limit	3,100,000	0.15
Experimental conditions	1,800,000	0.16

A passage diameter greater than four times these values would then isolate a thermocouple junction placed in the passage center from the effects of the gases cooled by the probe mount under both laminar and turbulent flow given the conditions listed in Table 1. Therefore, a thin-walled tube (wall thickness of approximately 1 mm) with an outer diameter equal to the probe stem was used for the passage (see Figure 3).

The probe stem was constructed of two metal parts. The inner steel tube was hollow so that a two-holed fused alumina tube could traverse the distance from the outside of the chamber tube (at room pressure) to near the junction position. The holes in the fused alumina tube served as electrically isolated conduits for the thermocouple wires from the junction to the outside of the simulator. The fused alumina tube was to be press-fit into the hole through the inner steel tube. The inner steel tube was threaded so that a nut could be used on the outside of the chamber tube wall to tighten the probe securely to the chamber tube wall.

The outer steel tube, resembling a tobacco pipe, was threaded on the interior along the long axis. This threaded surface mated with the corresponding threads on the outer diameter of the inner steel tube as shown in Figure 3. The thermocouple wires were then attached to the inner wall of the "bowl" part of the tube. The glue utilized for attachment of the wires was a clear nitrocellulose-based lacquer containing a polyester resin (fingernail polish). The lacquer was electrically insulating as well as providing a protective surface that isolated the thermocouple wires from the abrasive combustion gases. After usage, the lacquer was easily dissolved in solvent and the probe reused. It was noted that the lacquer did not ignite until the metal parts of the probe exceeded 150 °C. For the duration of the experiment, the probe *in masse* does not approach this temperature.

The "bowl" was layered several times with the lacquer to provide electrical isolation from the steel tube. The wires were then positioned and additional layers were added until the wires along the walls of the "bowl" were completely covered. The lacquer was also used to cover the holes in the fused alumina tube after the thermocouple wires were in place, thus providing a pressure seal around the thermocouple wires as they exited from the junction region.

2.2.2 Modified Mount. Unfortunately, the mount shown in Figure 3 contained some flaws that were evident in the first test in the simulator. The press-fit of the fused alumina tube was not sufficient to retain it in place during the pressurization of the flow chamber. The inner steel tube was therefore modified by enlarging the central hole so that the same lacquer that attached the thermocouple wires could be used to glue the fused alumina sheath in place. The other major flaw was the strength of the inner steel tube. After the first test the inner steel tube was badly bent and nearly severed at the wall of the chamber tube.

Since it was not desirable for the probe to have a large diameter (required for greater strength), and thereby, impose a large disturbance in the propellant bed, it was decided that a small stiffener be added to the probe near the chamber tube wall. This "adapter" is shown in Figure 4. To accommodate the adapter, the hole through the chamber tube wall was enlarged from 4.8-mm to 7.9-mm diameter. The inner steel tube was therefore reinforced along the portion of its length inside the chamber tube wall and the outer steel tube was also reinforced against a bending moment at the chamber tube wall. The assembled thermocouple probe is shown in Figure 5.

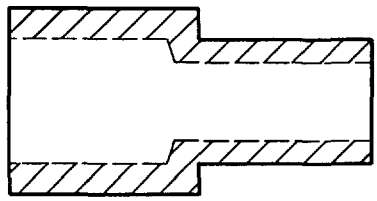

Figure 4. Cross-sectional view of stiffening adapter.

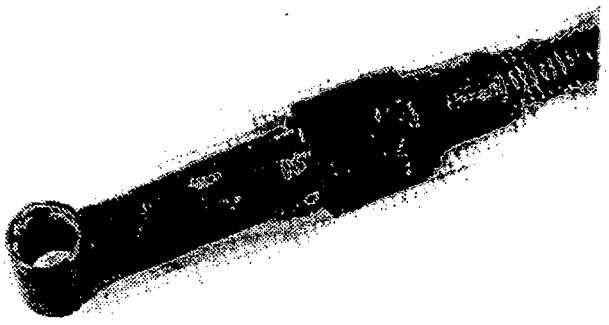

Figure 5. Photograph of assembled probe.

2.2.3 Double Thermocouple Mount. It was also desired to place two thermocouples of differing diameters in the same probe so that temperature sensitivities could be quantitatively compared. Otherwise, if the thermocouples were placed in two different probes, the same thermal environment for both thermocouple junctions could not be maintained. This uncertainty is almost assured in the random-packed propellant bed.

To accommodate the two thermocouples, the two-holed fused alumina tube was replaced with one with four holes (see Figure 6). Within the "bowl" region of the probe, one thermocouple was placed approximately 1 to 1.5 mm above the centerline of the fused alumina tube and the other placed at about the same distance below the centerline. This separation distance provided at least 20 junction-bead diameters between thermocouple junctions. At this distance, it was anticipated that flow eddies from the wake in the gases behind the first thermocouple would not disturb the second thermocouple. Later testing confirmed this assumption. The same temperature responses were obtained with the larger diameter thermocouple in front of as well as behind the smaller thermocouple.

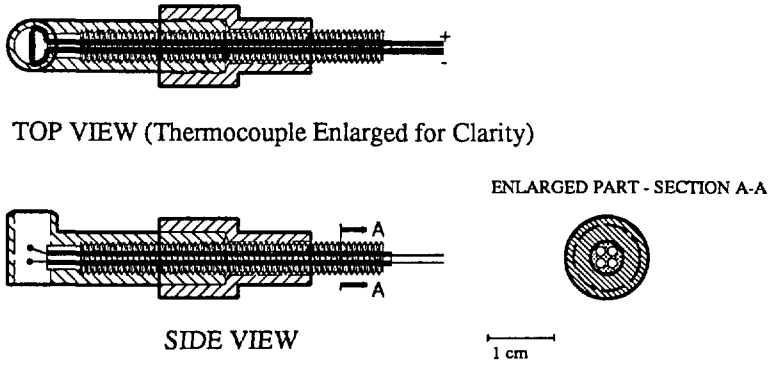

Figure 6. Cross-sectional view of modified thermocouple probe showing double thermocouples.

2.3 Thermocouple Corrections. Voltage values obtained from the thermocouples are subject to several possible corrections before an accurate temperature value can be assigned. The following sections describe each correction, its magnitude, and importance to this experiment.

2.3.1 Reference Temperature. Thermocouples produce a voltage essentially proportional to the temperature difference between the hot and cold junctions of two dissimilar metals (Seebeck effect). To assign a temperature to one of the junctions, the temperature of the other junction must be known. For noncryogenic work, the hot junction is used to determine the desired temperature and, therefore, the temperature of the cold junction must be known. Often a liquid/solid ice bath of known constant temperature into which the cold junction is immersed provides this reference. For these experiments, however, an electrically compensated circuit (electronic ice point) containing a temperature-sensitive resistor was inserted into the circuit between the amplifier and the hot thermocouple junction. This circuit was referenced to 0 °C and, therefore, provided a nearly constant correction of approximately 25 °C that removed the influence of ambient temperature in the range area. This correction was the only analog correction used; other corrections were applied to the voltage levels after their digital value was determined.

2.3.2 Catalytic Effects. An unfortunate side effect of using metals for temperature measurement at elevated temperatures is the effect of their catalytic nature upon the heated medium. If the metals contact gases that can combine exothermally on the surface of the thermocouple, the indicated temperature will be higher than that actually present in the gases. A common practice to avoid catalytic effects is to cover the thermocouple wire with an inert coating (Kent 1970). In addition to increasing the chemical inertness, such coatings increase the time response of the thermocouple. The emissivity of the coating over the temperature range also needs to be determined for radiative cooling corrections to be applied (see Section 2.3.3). However, if catalytic activity on the thermocouple junction is large, a coating must be applied. This section determines if this correction is large enough to be a concern for these types of experiments.

Estimates of the potential catalytic effects were obtained by assuming that the controlling reaction rate was limited by the flow across the thermocouple junction. Since the heating rate is further reduced by diffusion to and from the surface as well as a finite reaction time, this estimate should provide an indication of the maximum error. Another primary assumption was that the major heat source from catalytic heating (defined as excess heat) was derived from reactions with radicals such as hydrogen atoms (H) and not from the major neutral species (major species should be near equilibrium values before contacting the thermocouple junction and are therefore of low potential for catalytic heating).

Estimated concentrations of gaseous species at equilibrium produced by reacted igniter ball propellant (see Table 3 for H-atom concentrations), M30A1 (see Table 4 for H-atom concentrations) and M43 (see Table 5 for H-atom concentrations) were obtained from a NASA-Lewis equilibrium code (Gordon and McBride 1976) run on a PC platform. The pressure for the calculations was 3 MPa (see Kooker, Howard, and Chang 1993) and the temperature was varied by increments of 100 over the range from 300 K to 2400 K. As expected, the greatest concentrations of most radicals were found at higher temperatures. For example, the most prominent radical, H-atom, is present at a mole fraction of approximately 10^{-3} for all three propellants at a temperature of 2400 K.

Table 3. Ball Powder H-Atom Concentrations

Temperature (K)	Mole Fraction	ΔT Increase
700	0	
800	6.4×10^{-14}	4×10^{-11}
900	4.0×10^{-12}	3×10^{-9}
1000	1.1×10^{-10}	8×10^{-8}
1100	1.6×10^{-9}	1×10^{-6}
1200	1.3×10^{-8}	9×10^{-6}
1300	7.4×10^{-8}	5×10^{-5}
1400	3.2×10^{-7}	2×10^{-4}
1500	1.1×10^{-6}	8×10^{-4}
1600	3.4×10^{-6}	0.002
1700	9.0×10^{-6}	0.007
1800	2.1×10^{-5}	0.02
1900	4.7×10^{-5}	0.04
2000	9.5×10^{-5}	0.08
2100	1.8×10^{-4}	0.1
2200	3.2×10^{-4}	0.3
2300	5.4×10^{-4}	0.5
2400	8.9×10^{-4}	0.8

Note: Concentrations of less than 10^{-14} were rounded to zero.

Table 4. M30A1 H-atom Concentrations

Temperature (K)	Mole Fraction	ΔT Increase
700	0	
800	8.0×10^{-14}	6×10^{-11}
900	4.7×10^{-12}	4×10^{-9}
1000	1.2×10^{-10}	8×10^{-8}
1100	1.7×10^{-9}	1×10^{-6}
1200	1.3×10^{-8}	9×10^{-6}
1300	7.5×10^{-8}	6×10^{-5}
1400	3.2×10^{-7}	2×10^{-4}
1500	1.1×10^{-6}	7×10^{-4}
1600	3.5×10^{-6}	0.002
1700	9.2×10^{-6}	0.006
1800	2.2×10^{-5}	0.01
1900	4.8×10^{-5}	0.03
2000	9.8×10^{-5}	0.06
2100	1.9×10^{-4}	0.1
2200	3.3×10^{-4}	0.2
2300	5.7×10^{-4}	0.4
2400	9.3×10^{-4}	0.6

Table 5. M43 H-atom Concentrations

Temperature (K)	Mole Fraction	ΔT Increase
700	0	
800	7.4×10^{-14}	5×10^{-11}
900	4.3×10^{-12}	3×10^{-9}
1000	1.1×10^{-10}	1×10^{-7}
1100	1.6×10^{-9}	1×10^{-6}
1200	1.5×10^{-8}	9×10^{-6}
1300	9.1×10^{-8}	6×10^{-5}
1400	4.1×10^{-7}	3×10^{-4}
1500	1.5×10^{-6}	0.001
1600	4.5×10^{-6}	0.003
1700	1.2×10^{-5}	0.008
1800	2.9×10^{-5}	0.02
1900	6.5×10^{-5}	0.04
2000	1.3×10^{-4}	0.09
2100	2.5×10^{-4}	0.2
2200	4.6×10^{-4}	0.3
2300	7.8×10^{-4}	0.5
2400	1.3×10^{-3}	0.9

Given that H-atom was the most abundant radical, its catalytic activity on a platinum-containing surface is high and that recombination to form molecular hydrogen is one of the radical reactions that produce the most heat, the heat from catalytic effects was approximated from its concentration. This estimation assumed unit efficiency for the reaction at every available site on the surface of the junction bead. Therefore, every collision of H-atom on the surface produced heat. The collision rate was obtained from the kinetic theory of gases (Alberty and Daniels 1979) using the following expression:

$$\xi = \frac{P}{\left[\frac{2\pi RT}{M}\right]} \qquad (4)$$

where ξ is the collision rate, P is the pressure, R is the universal gas constant and M is the molecular weight of the gas mixture. The enthalpy of reaction was then calculated from the product of the heat of reaction (taken to be ΔH_f of H-atom [Weast and Astle 1980]), the

collision rate, the residence time of the gas at the junction (τ), the mole fraction of H-atom (X) and the surface area (A) as shown in Equation 5 (N, the Avogadro constant, is used to standardize units).

$$\Delta H_r = \Delta H_f\left[\frac{\xi}{N}\right]\tau XA \qquad (5)$$

The residence time was taken as the amount of time that a gas molecule in the flow stream would spend in the vicinity of the junction assuming viscous flow over the junction with only small wake eddies (i. e., linear flow speed divided by the diameter of the junction).

The deviation from the "true" temperature (from 300 K to 2400 K by increments of 100 K) then was determined by dividing the enthalpy of reaction by the heat capacity and mass of the junction as in Equation 6,

$$\Delta T = \frac{\Delta H_r}{mC_p} \qquad (6)$$

where ΔT is the temperature difference in Kelvin, ΔH_r is the enthalpy of reaction, m is the mass of the thermocouple junction and C_p is the heat capacity of the thermocouple junction.

After utilizing the approximation that H-atom recombination is the dominant reaction, the procedure was repeated using the larger set of reactions in Table 6 (H-atom recombination also included) with the heat of reaction released per gram mole of limiting reactant listed as ΔH. The contribution for each reaction to the total enthalpy released diminishes in order of its presentation in the table. Other reactions were considered but the concentrations of the necessary species were not great enough to warrant inclusion in the list. With the listed reactions included, the temperature differences were approximately less than double those calculated with solely H-atom concentrations. The greater temperature differences (in degrees Kelvin) for all energetic materials in this experiment are reported in Tables 3 to 5.

Table 6: Reaction Set for Computation of Catalytic Temperature Change

Reaction	ΔH (kcal/gmole)
$H + H \rightarrow H_2$	-104
$OH + H \rightarrow H_2O$	-119
$O + CO \rightarrow CO_2$	-128
$NH_2 + H \rightarrow NH_3$	-145
$CH_3 + H \rightarrow CH_4$	-104
$2NO + 2H_2 \rightarrow N_2 + H_2O$	-101

For all investigated temperatures, the deviation in temperature was estimated as less that 1 K. It appears that the small residence time of the event is responsible for the small value of the temperature increase. The value of 1 K is less than the manufacturer's uncertainty for this type of thermocouple. Therefore, catalytic effects were ignored for this experiment.

2.3.3 Radiative Effects. Another correction to be applied is that for radiative cooling of the hot junction in the flowing gases. This correction is approximated by assuming a quasisteady-state condition in which the electronic states of the junction material communicate readily with the vibrational modes in the crystalline material. As thermal energy is imparted to the junction, it randomizes rapidly and causes excitation of the electronic states which subsequently relax by photon emission. Loss of energy by radiation then cools the junction. Inherent in the derivation of the corrective term is the assumption that a sufficient length of thermocouple wire on both sides of the junction is on or nearly on the same isotherm as the junction so that conduction losses from the junction through the thermocouple wires are essentially zero. The remaining energy terms (e. g., energy transferred convectively to the thermocouple from the gases and energy lost by radiation) are set equal to each other and the corrective term obtained. For a spherical junction bead this term is given by (Hayhurst and Kittleson 1977; Peterson 1981)

$$\Delta T = T_{cal} - T_{obs} = \frac{\varepsilon \sigma d \left(T_{obs}^{\ 4} - T_o^{\ 4} \right)}{2k} \qquad (7)$$

where ε is the emissivity of the coated thermocouple (taken to be near 0.1 below 1000 °C and 0.2 near 1500 °C [Weast and Astle 1980]), σ is the Stefan-Boltzmann constant, d is the diameter of the junction, k is the thermal conductivity of the gases present at the sampling region and T_0 is approximately 300 K. The thermal conductivity was obtained as a function of temperature using empirical expressions (Liley and Gambill 1973) and corrected for gas composition as approximated by the NASA-Lewis code. Thus, a lower limit of 8×10^{-5} cal sec^{-1} cm^{-1} K^{-1} was obtained for the current example. The diameter of the thermocouples was estimated to be approximately double that of the wire diameter. The magnitude of the correction for the thermocouples was computed to be approximately 30 K in the region of peak temperature for each of the three propellants for a 1-mil (25 μm) diameter thermocouple.

2.4 Estimate of Thermocouple Time Constants. For the temperature measurement to have meaning during a transient event, the lag time must be sufficiently smaller than the transient time. This lag time can be associated with the volume and mass of the sensing element. The larger and heavier the element, the greater is the lag time. Therefore, the smallest sensing element available would appear to be most acceptable. However, the element must be sufficiently strong to survive the event of interest. For these experiments, the transient time is on the order of the time required for the diaphragm to break and the gas pressure in the flow chamber to plateau. Pressure measurements have established the value of the transient time in the range of 2 to 3 milliseconds (see Kooker, Chang, and Howard 1993; Kooker, Howard, and Chang 1993).

For an element immersed in a rapidly moving fluid such as is present in the flow chamber, the detection of temperature is closely coupled with convective heat transfer. The lag time is inversely proportional to the convective heat transfer coefficient and is decreased as the coefficient becomes larger. The following descriptive equations are valid for a single spherical element immersed in the fluid flow (Knudsen et al. 1973; Liley and Gambill, 1973):

$$N_{Pr} = C_p\left(\frac{\mu}{k}\right) \tag{8}$$

$$Re_s = \frac{\rho v d}{\mu} \tag{9}$$

$$N_{Nu} = 2 + 0.6(Re_s)^{1/2}(N_{Pr})^{1/3} \tag{10}$$

$$h = \frac{N_{Nu} k}{d} \tag{11}$$

and (Baker, Ryder, and Baker 1975)

$$\varpi = \frac{cd}{4h} \tag{12}$$

where N_{Pr} is the Prandlt number for the fluid, Re_s is the Reynolds number for the undisturbed free stream, N_{Nu} is the Nusselt number, h the convective heat transfer coefficient, c is the volumetric heat capacity for the thermocouple junction and ϖ is the lag time. The characteristic length for all the dimensionless parameters is the diameter of the sphere, d, and the fluid properties are evaluated at the film temperature, $(T_s + T_\infty)/2$. The lag time is defined as the amount of time required for the sensing element to come within $1/e$ of the temperature (e is the base for Naperian logarithms). For the element to achieve 99.3 % or greater response, the total time will be in excess of 5ϖ.

Since M30A1 is to be used as a base case for further experiments, the lag times reported in Table 7 were obtained using equilibrium property data for this propellant. Lag times for both M43 and the igniter ball powder were approximately 10% less. Based on the pressure-time histories obtained by Kooker and coworkers (Kooker, Chang, and Howard 1993; Kooker, Howard, and Chang 1993), it is easily evident in Table 7 that the lag time for a 3-mil (76 μm) thermocouple is unacceptably long for this experiment. The 2-mil (51 μm) thermocouple should show some blurring of detail near peak temperatures and the 1-mil (25 μm) thermocouple should be adequate throughout the entire temperature range if it can survive the ballistic event.

Table 7: Lag Times for Thermocouples[†]

Propellant	3-mil (76 μm)	2-mil (51 μm)	1-mil (25 μm)
M30A1	3.0	1.5	0.4
M43	2.7	1.4	0.4
Ball Powder	2.6	1.3	0.3

[†]Times in milliseconds

3. RESULTS AND DISCUSSION

3.1 Inert Propellant Beds. Prior to utilization of live propellant in the flow chamber, the simulator was tested with inert propellant. During these tests, the stiffening adapter was added because the thermocouple probes were moving in the chamber as the inert propellant compressed. This movement was sufficient to shear several probes at the tube wall. After addition of the adapter, the probes were used several times before replacing the thermocouple wire and the probe itself showed little or no damage.

After the mounting of the thermocouple wire and the probe proved adequate, it was desired to directly compare results from different diameter thermocouples. However, the vagaries of fluid flow through an agglomerate bed negated the possibility of obtaining exactly the same fluid conditions, and hence, the same temperature sensing properties in two or more different experimental runs that would be necessary for thermocouple performance comparison. Therefore, it was decided to place both thermocouples in the same mount with sufficient separation distance to prevent wake disturbances in the second thermocouple. The double thermocouple probe was designed (see Figure 6) to accomplish these goals and to determine the thermocouple diameter that would demonstrate a sufficiently short lag time. The first comparison was with 3-mil (76 μm) and 2-mil (51 μm) thermocouples. The thermocouple comparisons reported here are from the upper position in the flow chamber (see T1 in Figure 1). Figure 7 shows a typical temperature-history trace when the flow chamber contains inert propellant simulant grains and the ignition was created by combustion of ball propellant in the igniter chamber.

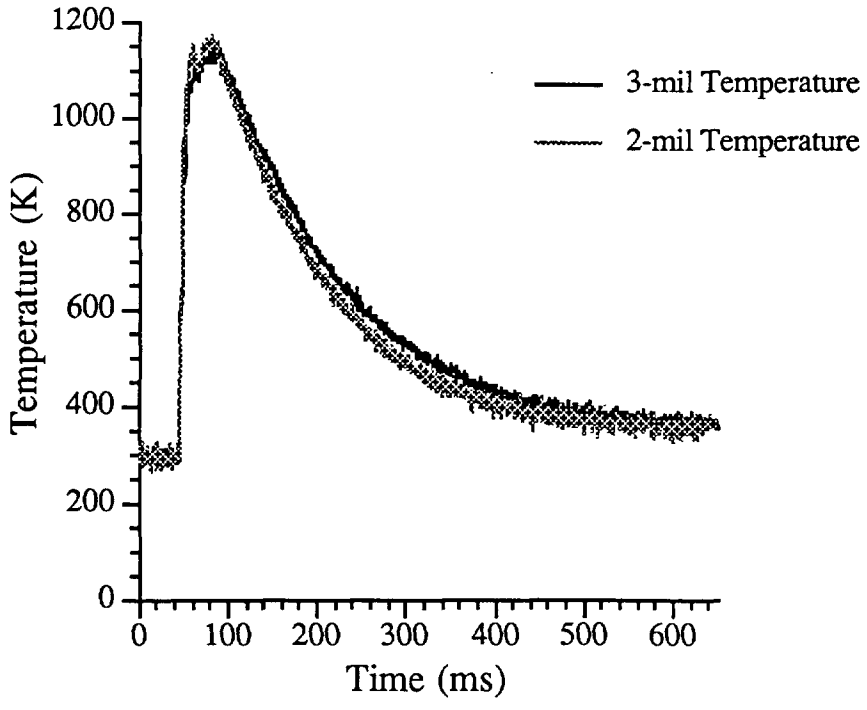

Figure 7. Comparison of temperature-history traces of 3-mil (76 μm) and 2-mil (51 μm) thermocouples (with inert propellant).

Since the pressure burst of hot gases through the diaphragm is approximately a step function, it is not surprising that both thermocouples initially respond in a similar fashion. However, they soon begin to show differences in response and above 1000 K the measurements begin to show significant differences. At this temperature, the 3-mil (76 μm) thermocouple lags and reports lower temperatures. As time progresses, the reading for the 2-mil (51 μm) thermocouple drops below that of the 3-mil (76 μm) thermocouple. At long time, after approximately 600 ms, the two traces come together. This behavior is indicative of the greater heat transfer coefficient for the 2-mil (51 μm) thermocouple (estimated at 30 kJ m^{-2} s^{-1} K^{-1}) than for the 3-mil (76 μm) thermocouple (estimated at 20 kJ m^{-2} s^{-1} K^{-1}). During the heating phase, the 2-mil (51 μm) thermocouple heats faster, and hence, during the cooling phase, it also cools faster. When the thermal environment is static and convection no longer is the dominant heat transfer term, the readings are identical. Figure 8 shows this effect more clearly (positive values during the heating phase and negative during the cooling phase). The maximum deviation is approximately 80 K during the heating phase and 50 K during the cooling phase.

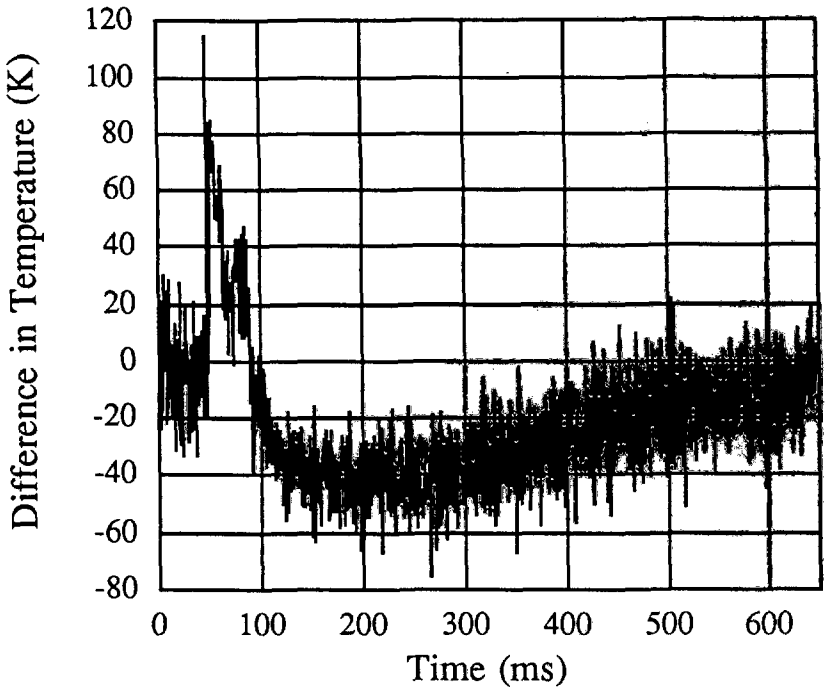

Figure 8. Difference of temperature-history traces of 3-mil (76 μm) and 2-mil (51 μm) thermocouples (with inert propellant).

When the 1-mil (25 μm) thermocouple (with a convective heat transfer coefficient estimated at 50 kJ m^{-2} s^{-1} K^{-1}) was compared with the 2-mil (51 μm) thermocouple, the same type behavior between thermocouples was noted. Figure 9 demonstrates the higher temperature reading for the 1-mil (25 μm) thermocouple during the heating phase and lower temperatures during the cooling phase. If the differences, as computed in Figure 10, are added to those of Figure 8, temperature differences of greater than 200 K between 3-mil (76 μm) and 1-mil (25 μm) thermocouples would be obtained. These differences in response are too great to allow usage of the 3-mil (76 μm) thermocouple in describing the thermal environment. Therefore, the 3-mil (76 μm) thermocouple was not used. While the 1-mil (25 μm) thermocouple appears to be the best choice with respect to lag time, the 2-mil (51 μm) thermocouple was chosen for tests with live propellant because it was stronger than the 1-mil (25 μm) thermocouple and more likely to survive the stronger pressurization wave.

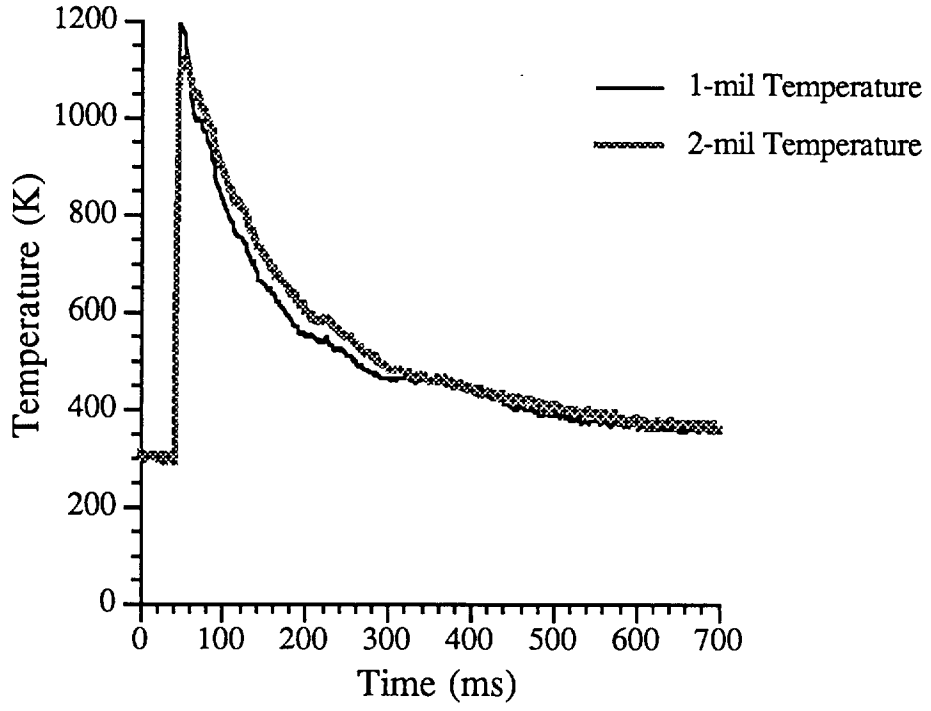

Figure 9. Comparison of temperature-history traces of 2-mil (51 μm) and 1-mil (25 μm) thermocouples (with inert propellant).

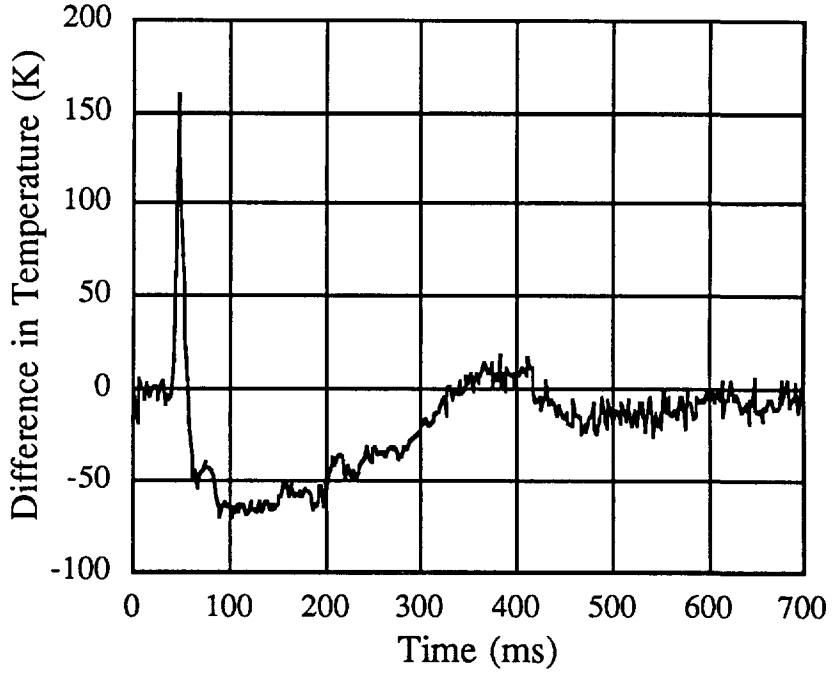

Figure 10. Difference of temperature-history traces of 2-mil (51 μm) and 1-mil (25 μm) thermocouples (with inert propellant).

3.2 Live Propellant Beds. After characterization of the thermocouples in an inert propellant bed, two different live propellants were tested in the flow chamber. Triple-base M30A1 was chosen as a baseline case because it exhibits a vigorous visible flame zone at or close to the propellant surface at the pressures expected in the flow chamber. M43, on the other hand, burns with a visible flame zone detached from the surface of the propellant. There appears to be a "dark" or induction zone that delays ignition of the gases evolving from the propellant (Vanderhoff, Anderson, and Kotlar 1992; Miller 1992). Further studies beyond the scope of this report will be performed to ascertain the effect of the induction zone during the ignition sequence of these propellants.

For the present experiments, the sizes of the propellant grains were not identical (see Table 8 and Figure 11) due to availability. However, important information was revealed with the presence of the thermocouples in the propellant bed.

Preliminary tests (see Kooker, Howard, and Chang 1993) with live propellant demonstrated the need for a small inert propellant layer at the top of the propellant bed. This region is very close to the nozzle plate and is, therefore, subject to the shock boundaries from the merging high-pressure jets emanating therefrom. To prevent contact of these shock boundaries with the live propellant and thus avoid spurious ignition, a thin layer of inert propellant was added to the top of the bed.

Table 8: Properties of Solid Propellant Grains

Propellant Property	Inert Grains	M30A1 Grains	M43 Grains
Length (mm)	24.3	28.5	13.9
Diameter (mm)	10.7	12.3	8.4
Perforation Diameter (mm)	0 (solid)	1.23	1.35
Density (g/cc)	1.60	1.67	1.65

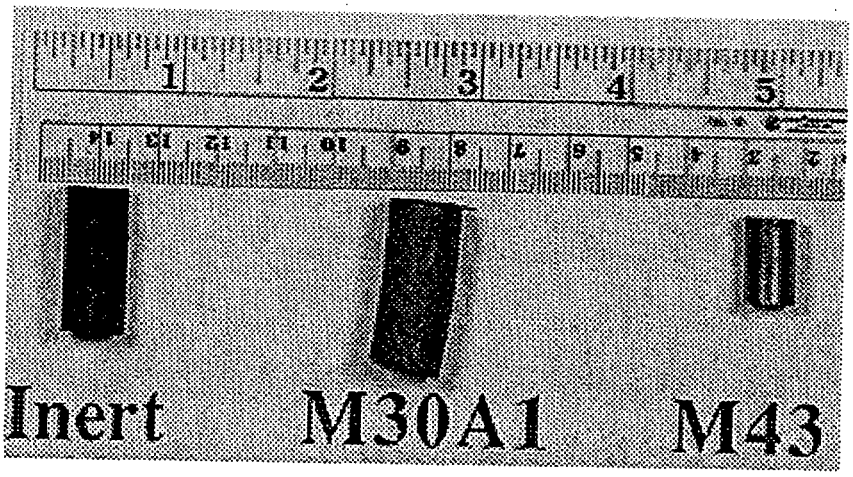

Figure 11. Photograph of propellants used.

With these precautions, a smooth temperature history such as that shown in Figure 12 is obtained (thermocouple locations as shown in Figure 1 with T1 as the upper thermocouple and T2 as the lower). The temperature rapidly increases from ambient to about 1200 K at the location of the upper thermocouple probe as the pressure wave from the igniter chamber (generated by the hot combustion products from that chamber) fills the flow chamber. The temperature then rises slowly suggesting propellant pyrolysis with minor energy release. During the next few milliseconds (commencing approximately 15 ms after pressurization of the chamber), ignition becomes more rapid with runaway ignition above 2000 K. The lower thermocouple probe detected similar behavior. The temperatures were, however, lower until runaway ignition occurred nearly 20 ms after chamber pressurization.

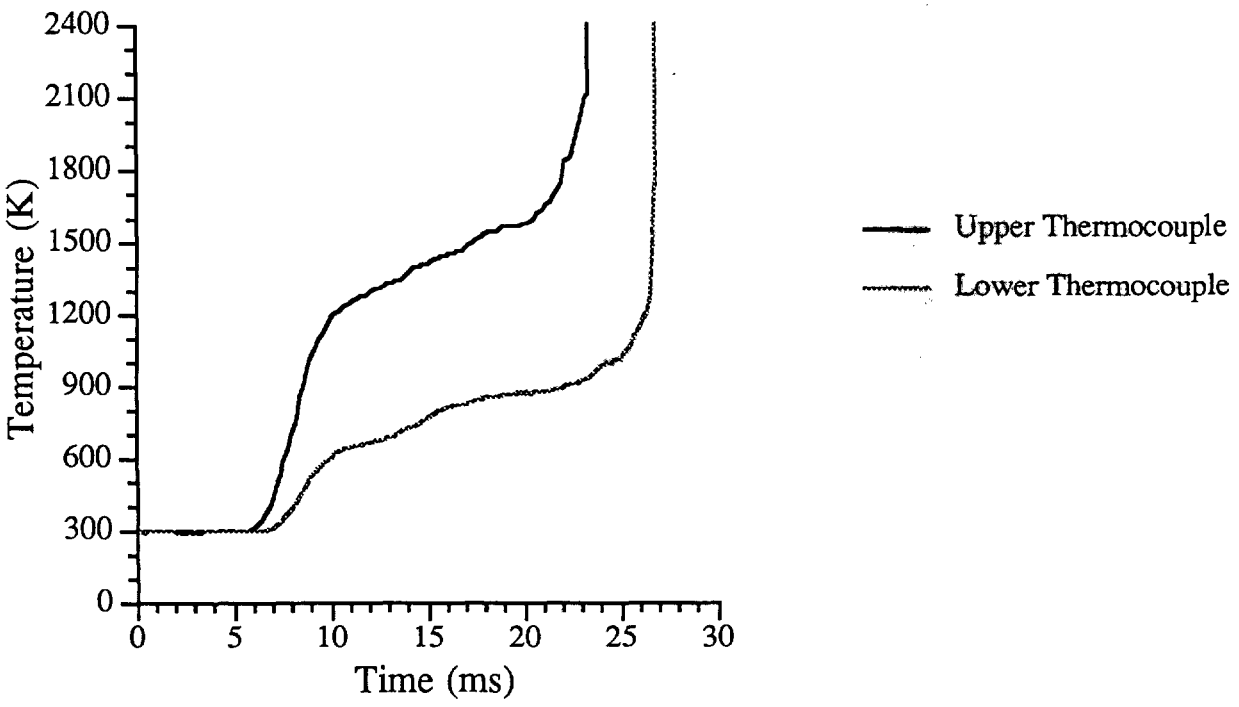

Figure 12. Temperature-history traces of upper and lower thermocouples with M30A1 propellant.

Ignition of M43 propellant under the same conditions as for M30A1 showed similar gross behavior (that is, rapid increase, plateau and runaway regions, for details see Figure 13). However, important details are different. Most prominent is the temperature excursion that occurs in the early phase of chamber pressurization. The upper thermocouple momentarily attained 1900 K and the lower thermocouple 2400 K or greater (inclusion of the radiative correction factor extends the thermocouple limit to 2630 K). It is not known if the lower thermocouple was damaged during the excursion. In this particular experiment, both thermocouples picked up 60 Hz noise that required signal deconvolution. The residual from the lower thermocouple trace still retains evidence of the noise and, therefore, is somewhat suspect.

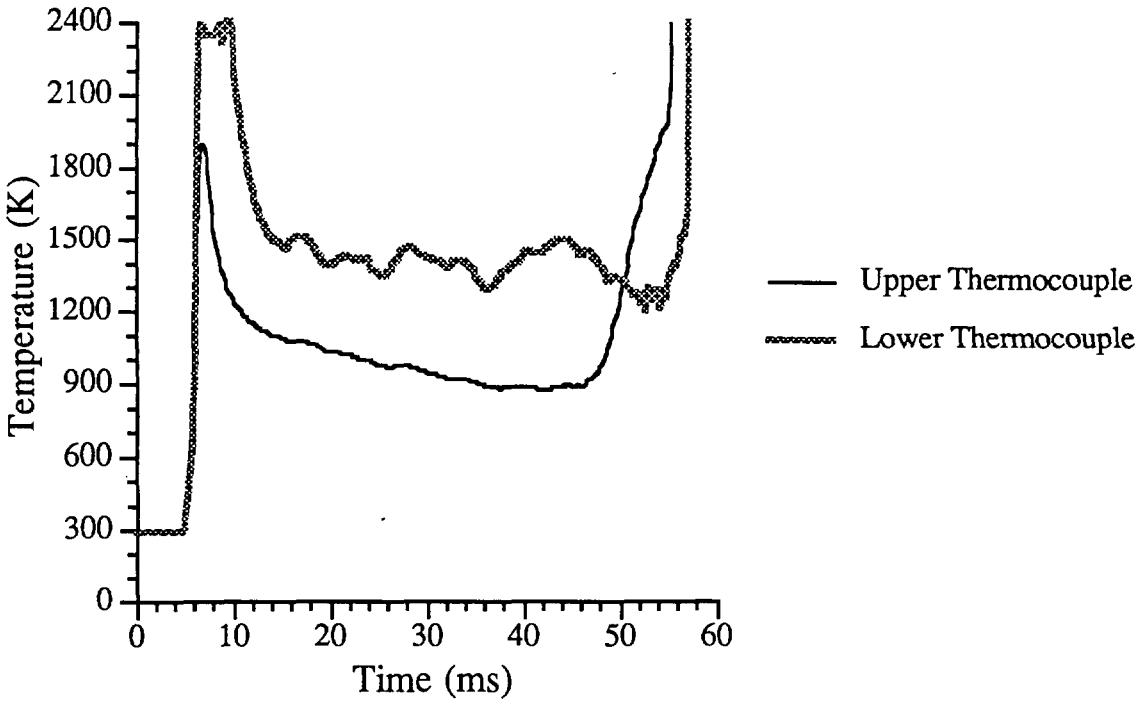

Figure 13. Temperature-history traces of upper and lower thermocouples with M43 propellant.

After the initial exothermal response from the propellant, the temperature decreased to about 1200 K and then slowly declined to about 900 K. During this time, about 40 ms, a "hang-fire" ignition occurred. In other words, the propellant received the ignition stimulus and appeared not to react during a long induction period. At the end of this period, combustion rapidly took place throughout the propellant bed and in less than 10 ms the thermocouples reported thermal runaway. During the runaway, the chamber pressure also rapidly increased until sufficient pressure was generated to activate the rupture disk and eject the burning propellant into the waiting water bath for quenching of the remaining propellant.

4. SUMMARY

Platinum versus 10% Rh/platinum fine-wire thermocouple were used to obtain gas-phase temperatures within a propellant bed. Probe mounts that provided sufficient physical support for the fine-wire thermocouples and minimally perturbed the flow environment were designed and evaluated. Different thermocouple wire diameters also were evaluated for their response (lag) times. Two thermocouples of differing diameter were placed in the same probe mount so that the same thermal environment was sampled by both. This configuration was evaluated for systemic errors. No apparent biasing of the measurement was noted. The largest diameter thermocouple (3 mil or 76 μm) exhibited a response time too great for determining temperatures during the ignition phase of a propellant bed. The smallest diameter (1 mil or 25 μm) exhibited the shortest response time and would be the thermocouple of choice for this experiment; however, it was not used in the current experiments due to difficulties in probe fabrication and consideration of the wire strength. The 2-mil (51 μm) wire was judged adequate except possibly during the very early heating phase in which the temperature rises very rapidly (in this case, an event that approximated a step function).

Theoretically (Equations 8-12), each succeeding smaller diameter will show a deviation from the larger diameter during times of rapid gas movement because the convective heat transfer coefficient varies with the inverse of approximately the square root of the diameter. As the gas velocity diminishes and heat transfer is controlled primarily by conduction, the indicated temperatures of both large and small thermocouples become equal. Implicit in Equation 12 are two extensive properties of the thermocouple junction that affect the lag time. Namely, the product of the volumetric heat capacity and the junction diameter reflects the ratio of the mass of the junction to its surface area. As the mass (diameter) of the junction increases, so does the lag time. However, as the surface area that is presented for heat transfer increases, the lag time decreases. Therefore, the ideal junction should consist of the least amount of mass but should present a maximum surface area to the gas flow. Both these conditions make a thermocouple junction that is weak and would not survive a rapid gas flow. Thus, a bargain is struck between extreme rapidity and surviving the event long enough to provide useful data.

The reporting difference due to convection during rapid gas flow was demonstrated by the indicated temperatures reported by both large and small thermocouples [reporting pairs of 3- and 2-mil diameter (76 and 51 μm) and of 2- and 1-mil (51 and 25 μm) diameter wires] in the double mount. At long times when the convective flow had diminished to essentially zero, the indicated temperatures by each member of the reporting pair asymptotically approached the same value.

Two sources of possible error in the thermocouple measurement (catalytic heating and radiative heat loss) were investigated and the magnitude of each error determined. Gas-phase concentrations of radicals were obtained via a NASA-Lewis equilibrium code and the maximum temperature due to catalytic reactions on the thermocouple surface determined. Temperature error due to catalytic effects was estimated to be less than 1 K and was subsequently ignored. Radiative corrections to the temperatures were mainly dependent on the thermocouple material and emissivity. These values were obtained from the thermocouple manufacturer. The experimental parameter related to the experiment was the gas mixture thermal conductivity. This property was estimated from engineering expressions that were corrected for composition by the NASA-Lewis equilibrium simulation code. The magnitude of the correction for the thermocouples was computed to be approximately 30 K in the region of peak temperature for each of the three thermocouples.

Tests with inert propellant beds indicated a peak gas temperature in the region of 1200 K at a pressure of approximately 3 MPa in the flow chamber. These conditions are thought to be representative of those present in some ignition systems. Preliminary tests also indicate that ignition characteristics are highly dependent upon the physical condition of the propellant bed and the manner of introduction of the hot gases into the bed. These results and others (see Kooker, Howard, and Chang 1993) show promise of tailoring the ignition stimulus so that different parameters of the hang-fire condition can be investigated.

5. REFERENCES

Alberty, R. A. and F. Daniels. Physical Chemistry, 5th edition, John Wiley & Sons, New York, 1979, Chapter 14.

Baker, H. D., E. A. Ryder, and N. H. Baker. Temperature Measurement in Engineering, vol. II, Omega Press, Stamford, Chapter 6, 1975.

Brosseau, T. L., I. C. Stobie, J. R. Ward, and R. W. Geene. "120 mm Gun Heat Input Measurements." ARBRL-TR-02413, U. S. Army Ballistic Research Laboratory, July 1982.

Brosseau T. L. and J. R. Ward. "Reduction of Heat Transfer in 105 mm Tank Gun by Wear-Reducing Additives." BRL-MR-2698, U. S. Army Ballistic Research Laboratory, November 1976.

Brosseau T. L. and J. R. Ward. "Measurement of the Heat Input into the 105 mm M68 Tank Cannon Firing Rounds Equipped with Wear-Reducing Additives." BRL-TR-02056, U. S. Army Ballistic Research Laboratory, April 1978.

Chang, L.-M., R. W. Deas, and J. Grosh. "Ignition Studies of Two-Piece Cartridges for an Advanced Tank Cannon System (ATACS)." BRL-TR-3249, U. S. Army Ballistic Research Laboratory, August 1991.

Chang, L.-M. and J. J. Rocchio. "Simulator Diagnostics of the Early Phase Ignition Phenomena in a 105-mm Tank Gun Chamber." BRL-TR-2890, U. S. Army Ballistic Research Laboratory, March 1988.

Gordon, S. and B. J. McBride. "Computer Program for Calculation of Complex Chemical Equilibrium Compositions, Rocket Performance, Incident and Reflected Shocks, and Chapman-Jouguet Detonations." NASA SP-273, NASA Lewis Research Center, March 1976.

Hayhurst, A. N. and D. B. Kittelson. "Heat and Mass Transfer Considerations in the Use of Electrically Heated Thermocouples of Iridium versus an Iridium/Rhodium Alloy in Atmospheric Pressure Flames." Combustion and Flame, vol. 28, p. 301, 1977.

Horst, A. W. "Multiphase Flow Analysis of the Ballistic Performance of an Anomalous LOVA Propellant Mix." 20th JANNAF Combustion Meeting, CPIA Publication 383, vol. I, p. 557, October 1983.

Horst, A. W. "Breechblow Phenomenology Revised." BRL-TR-2707, U. S. Army Ballistic Research Laboratory, January 1986.

Kent, J. H. "A Noncatalytic Coating for Platinum-Rhodium Thermocouples." Combustion and Flame, vol. 14, p. 279, 1970.

Klingenberg, G. and H. Mach. "Experimental Study of Non-Steady Phenomena Associated with the Combustion of Solid Gun Propellants." Proceedings of the 16th Symposium (International) on Combustion, Cambridge, Massachusetts, August 15-21, 1976.

Knudsen, J. G., K. J. Bell, A. D. Holt, H. C. Hottel, A. D. Sarofim, F. C. Standiford, D. Stuhlbarg, and V. W. Uhl. "Heat Transmission." Chemical Engineer's Handbook, 5th ed.; Perry, R. H.; Chilton, C. H. Eds., McGraw-Hill, New York, Section 10, 1973.

Kooker, D. E., L.-M. Chang, and S. L. Howard. "Flamespreading in Granular Solid Propellant: Design of an Experiment." ARL-MR-80, U. S. Army Ballistic Research Laboratory, June 1993.

Kooker, D. E., S. L. Howard, and L.-M. Chang. "Flamespreading in Granular Solid Propellant: Initial Results." 30th JANNAF Combustion Meeting, CPIA Publication 606, vol. I, November 1993.

Kracek, F. C. and W. J. Benedict. "Temperature of Propellant Gases." National Defense Research Committee, Armour and Ordnance Report No. A-201, July 1943.

Kracek, F. C. and W. J. Benedict. "An Experimental Study of Powder Gas Radiation and Temperature." National Defense Research Committee, Armour and Ordnance Report No. A-252, February 1944.

Liley, P. E. and W. R. Gambill. Chemical Engineer's Handbook, 5th ed.; Perry, R. H.; Chilton, C. H. Eds., McGraw-Hill, New York, 1973, Section 3.

May, I. W., and A. W. Horst. "Charge Design Considerations and Effect on Pressure Waves in Gun." ARBRL-TR-0277, U. S. Army Ballistic Research Laboratory, December 1978.

Miller, M. S. "Modeling of Kinetics and Combustion of Energetic Materials." ARO-URI Meeting on Fast Reaction Kinetics and Modeling of Energetic Material Combustion, The Pennsylvania State University, State College, PA, August 1992.

McClure, D. R. Measurement of Gas Temperature and Convective Heat Flux in a Reacting Granular Propellant Bed, Ph.D. Dissertation Thesis, Pennsylvania State University, Pennsylvania, 1984.

Penzias, G. J. "Temperature Measurement and Gas Analysis in Flames and Plasmas Using Spectroscopic Methods." Combustion Technology: Some Modern Developments, Palmer, E. and Y. Beer, Eds., Academic Press, New York, 1974.

Peterson, R. C. PhD Thesis, Purdue University, 1981.

Schlichting, H. Boundary Layer Theory, McGraw-Hill, New York, 1960a, p. 25.

Schlichting, H. Boundary Layer Theory, McGraw-Hill, New York, 1960b, p. 537.

Stobie, I. C., T. L. Brosseau, and R. P. Kaste. "Heat Measurements in 105 mm Tank Gun with M735 Rounds." ARBRL-TR-02265, U. S. Army Ballistic Research Laboratory, September 1980.

Tourin, R. H. Spectroscopic Gas Temperature Measurement, Elsevier Publishing Co., Amsterdam, 1966.

Vanderhoff, J. A., W. R. Anderson, and A. J. Kotlar. "Dark Zone Modeling of Solid Propellant Flames." 29th JANNAF Combustion Meeting, CPIA Publication 593, vol. II, p. 225, October 1992.

Weast, R. C. and M. J. Astle, Eds., CRC Handbook of Chemistry and Physics, CRC Press, Inc., Boca Raton, 1980.

3. RESULTS AND DISCUSSION

3.1 Inert Propellant Beds. Prior to utilization of live propellant in the flow chamber, the simulator was tested with inert propellant. During these tests, the stiffening adapter was added because the thermocouple probes were moving in the chamber as the inert propellant compressed. This movement was sufficient to shear several probes at the tube wall. After addition of the adapter, the probes were used several times before replacing the thermocouple wire and the probe itself showed little or no damage.

After the mounting of the thermocouple wire and the probe proved adequate, it was desired to directly compare results from different diameter thermocouples. However, the vagaries of fluid flow through an agglomerate bed negated the possibility of obtaining exactly the same fluid conditions, and hence, the same temperature sensing properties in two or more different experimental runs that would be necessary for thermocouple performance comparison. Therefore, it was decided to place both thermocouples in the same mount with sufficient separation distance to prevent wake disturbances in the second thermocouple. The double thermocouple probe was designed (see Figure 6) to accomplish these goals and to determine the thermocouple diameter that would demonstrate a sufficiently short lag time. The first comparison was with 3-mil (76 μm) and 2-mil (51 μm) thermocouples. The thermocouple comparisons reported here are from the upper position in the flow chamber (see T1 in Figure 1). Figure 7 shows a typical temperature-history trace when the flow chamber contains inert propellant simulant grains and the ignition was created by combustion of ball propellant in the igniter chamber.

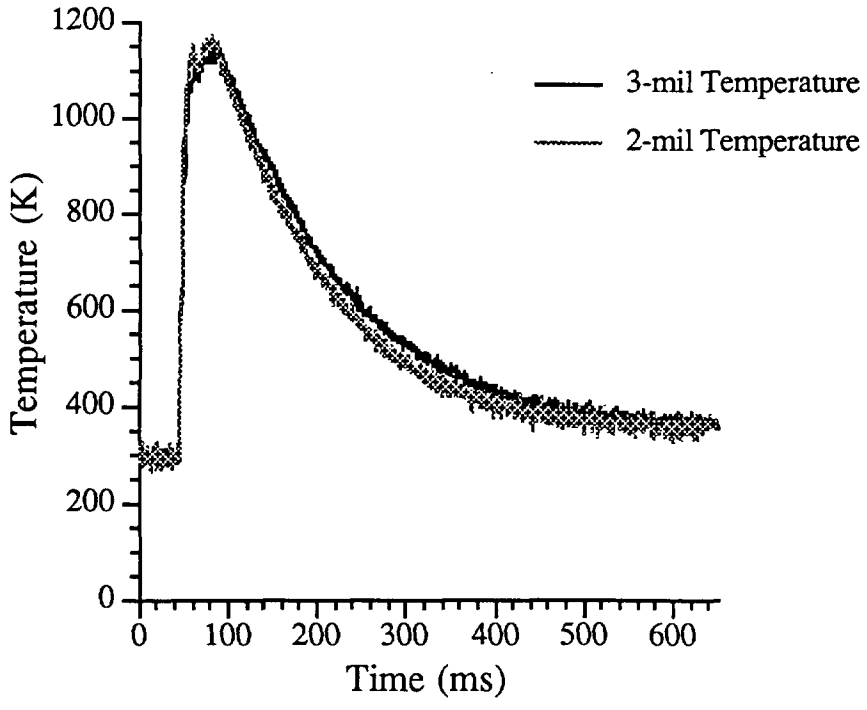

Figure 7. Comparison of temperature-history traces of 3-mil (76 μm) and 2-mil (51 μm) thermocouples (with inert propellant).

Since the pressure burst of hot gases through the diaphragm is approximately a step function, it is not surprising that both thermocouples initially respond in a similar fashion. However, they soon begin to show differences in response and above 1000 K the measurements begin to show significant differences. At this temperature, the 3-mil (76 μm) thermocouple lags and reports lower temperatures. As time progresses, the reading for the 2-mil (51 μm) thermocouple drops below that of the 3-mil (76 μm) thermocouple. At long time, after approximately 600 ms, the two traces come together. This behavior is indicative of the greater heat transfer coefficient for the 2-mil (51 μm) thermocouple (estimated at 30 kJ m^{-2} s^{-1} K^{-1}) than for the 3-mil (76 μm) thermocouple (estimated at 20 kJ m^{-2} s^{-1} K^{-1}). During the heating phase, the 2-mil (51 μm) thermocouple heats faster, and hence, during the cooling phase, it also cools faster. When the thermal environment is static and convection no longer is the dominant heat transfer term, the readings are identical. Figure 8 shows this effect more clearly (positive values during the heating phase and negative during the cooling phase). The maximum deviation is approximately 80 K during the heating phase and 50 K during the cooling phase.

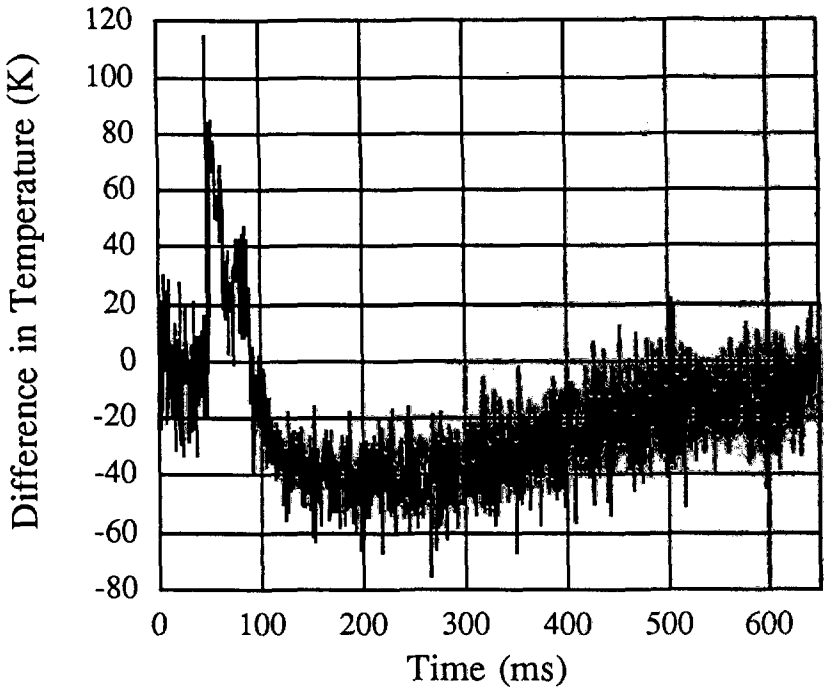

Figure 8. Difference of temperature-history traces of 3-mil (76 μm) and 2-mil (51 μm) thermocouples (with inert propellant).

When the 1-mil (25 μm) thermocouple (with a convective heat transfer coefficient estimated at 50 kJ m^{-2} s^{-1} K^{-1}) was compared with the 2-mil (51 μm) thermocouple, the same type behavior between thermocouples was noted. Figure 9 demonstrates the higher temperature reading for the 1-mil (25 μm) thermocouple during the heating phase and lower temperatures during the cooling phase. If the differences, as computed in Figure 10, are added to those of Figure 8, temperature differences of greater than 200 K between 3-mil (76 μm) and 1-mil (25 μm) thermocouples would be obtained. These differences in response are too great to allow usage of the 3-mil (76 μm) thermocouple in describing the thermal environment. Therefore, the 3-mil (76 μm) thermocouple was not used. While the 1-mil (25 μm) thermocouple appears to be the best choice with respect to lag time, the 2-mil (51 μm) thermocouple was chosen for tests with live propellant because it was stronger than the 1-mil (25 μm) thermocouple and more likely to survive the stronger pressurization wave.

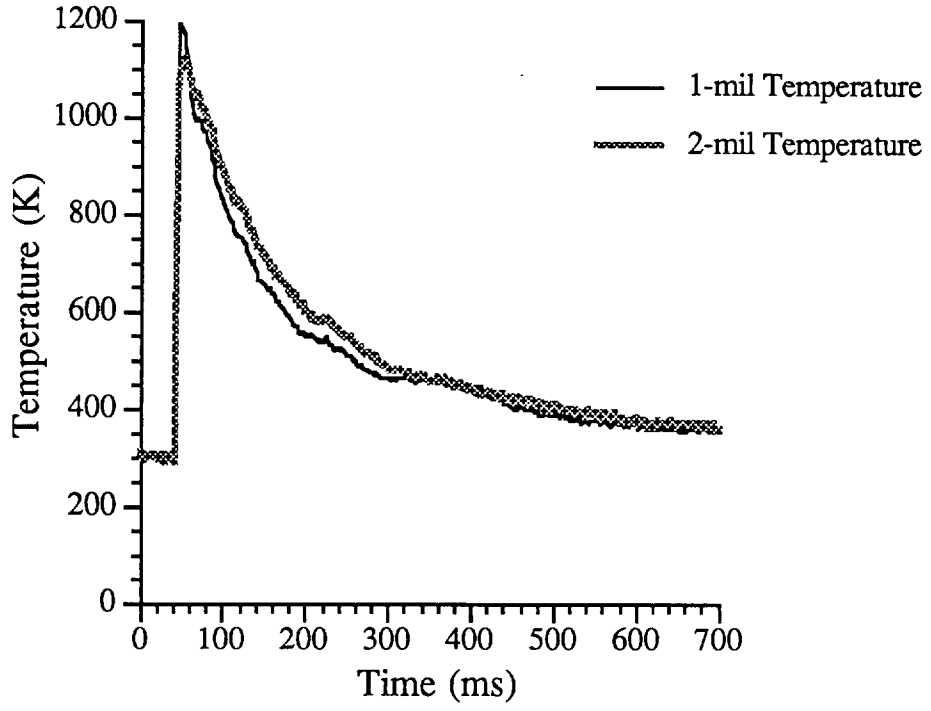

Figure 9. Comparison of temperature-history traces of 2-mil (51 μm) and 1-mil (25 μm) thermocouples (with inert propellant).

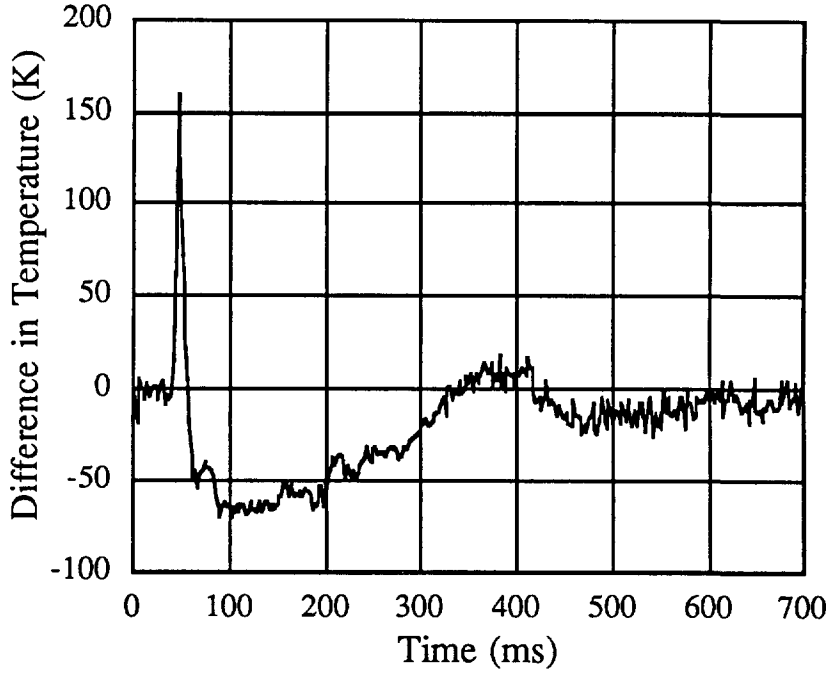

Figure 10. Difference of temperature-history traces of 2-mil (51 μm) and 1-mil (25 μm) thermocouples (with inert propellant).

3.2 Live Propellant Beds. After characterization of the thermocouples in an inert propellant bed, two different live propellants were tested in the flow chamber. Triple-base M30A1 was chosen as a baseline case because it exhibits a vigorous visible flame zone at or close to the propellant surface at the pressures expected in the flow chamber. M43, on the other hand, burns with a visible flame zone detached from the surface of the propellant. There appears to be a "dark" or induction zone that delays ignition of the gases evolving from the propellant (Vanderhoff, Anderson, and Kotlar 1992; Miller 1992). Further studies beyond the scope of this report will be performed to ascertain the effect of the induction zone during the ignition sequence of these propellants.

For the present experiments, the sizes of the propellant grains were not identical (see Table 8 and Figure 11) due to availability. However, important information was revealed with the presence of the thermocouples in the propellant bed.

Preliminary tests (see Kooker, Howard, and Chang 1993) with live propellant demonstrated the need for a small inert propellant layer at the top of the propellant bed. This region is very close to the nozzle plate and is, therefore, subject to the shock boundaries from the merging high-pressure jets emanating therefrom. To prevent contact of these shock boundaries with the live propellant and thus avoid spurious ignition, a thin layer of inert propellant was added to the top of the bed.

Table 8: Properties of Solid Propellant Grains

Propellant Property	Inert Grains	M30A1 Grains	M43 Grains
Length (mm)	24.3	28.5	13.9
Diameter (mm)	10.7	12.3	8.4
Perforation Diameter (mm)	0 (solid)	1.23	1.35
Density (g/cc)	1.60	1.67	1.65

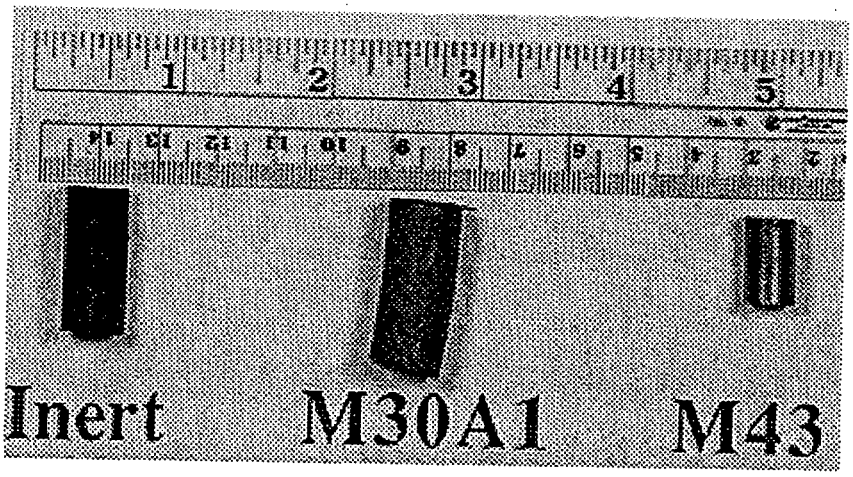

Figure 11. Photograph of propellants used.

With these precautions, a smooth temperature history such as that shown in Figure 12 is obtained (thermocouple locations as shown in Figure 1 with T1 as the upper thermocouple and T2 as the lower). The temperature rapidly increases from ambient to about 1200 K at the location of the upper thermocouple probe as the pressure wave from the igniter chamber (generated by the hot combustion products from that chamber) fills the flow chamber. The temperature then rises slowly suggesting propellant pyrolysis with minor energy release. During the next few milliseconds (commencing approximately 15 ms after pressurization of the chamber), ignition becomes more rapid with runaway ignition above 2000 K. The lower thermocouple probe detected similar behavior. The temperatures were, however, lower until runaway ignition occurred nearly 20 ms after chamber pressurization.

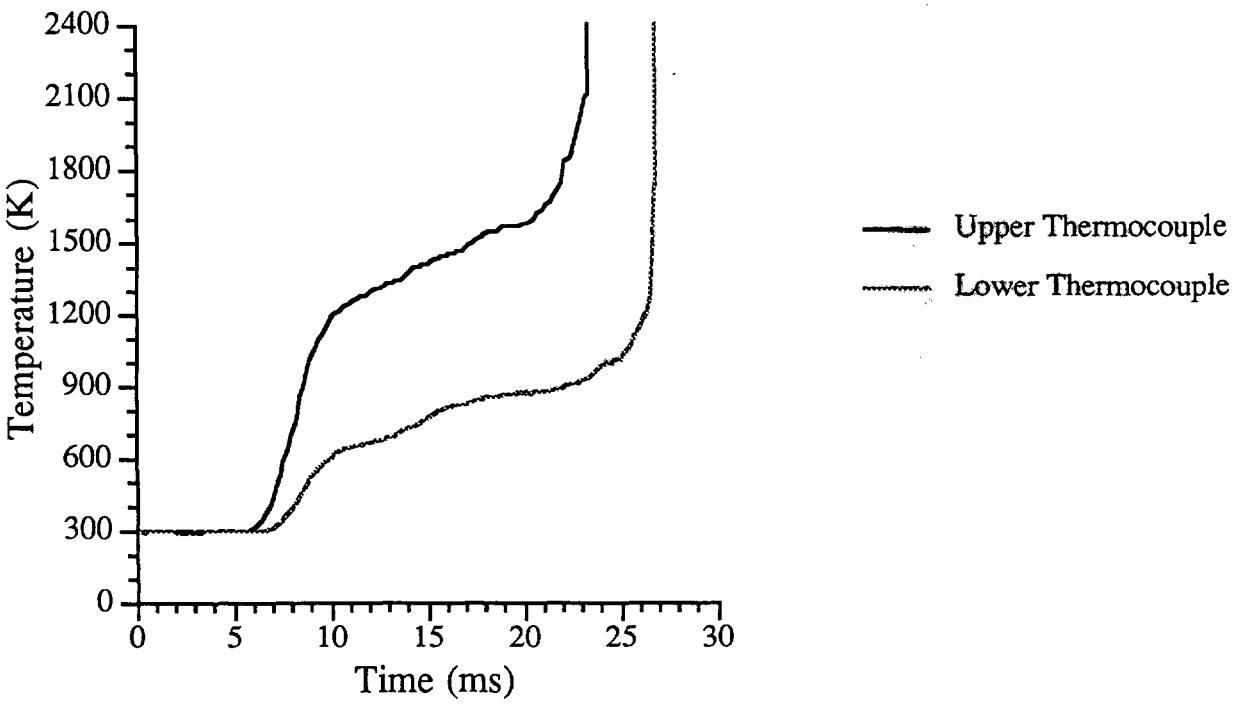

Figure 12. Temperature-history traces of upper and lower thermocouples with M30A1 propellant.

Ignition of M43 propellant under the same conditions as for M30A1 showed similar gross behavior (that is, rapid increase, plateau and runaway regions, for details see Figure 13). However, important details are different. Most prominent is the temperature excursion that occurs in the early phase of chamber pressurization. The upper thermocouple momentarily attained 1900 K and the lower thermocouple 2400 K or greater (inclusion of the radiative correction factor extends the thermocouple limit to 2630 K). It is not known if the lower thermocouple was damaged during the excursion. In this particular experiment, both thermocouples picked up 60 Hz noise that required signal deconvolution. The residual from the lower thermocouple trace still retains evidence of the noise and, therefore, is somewhat suspect.

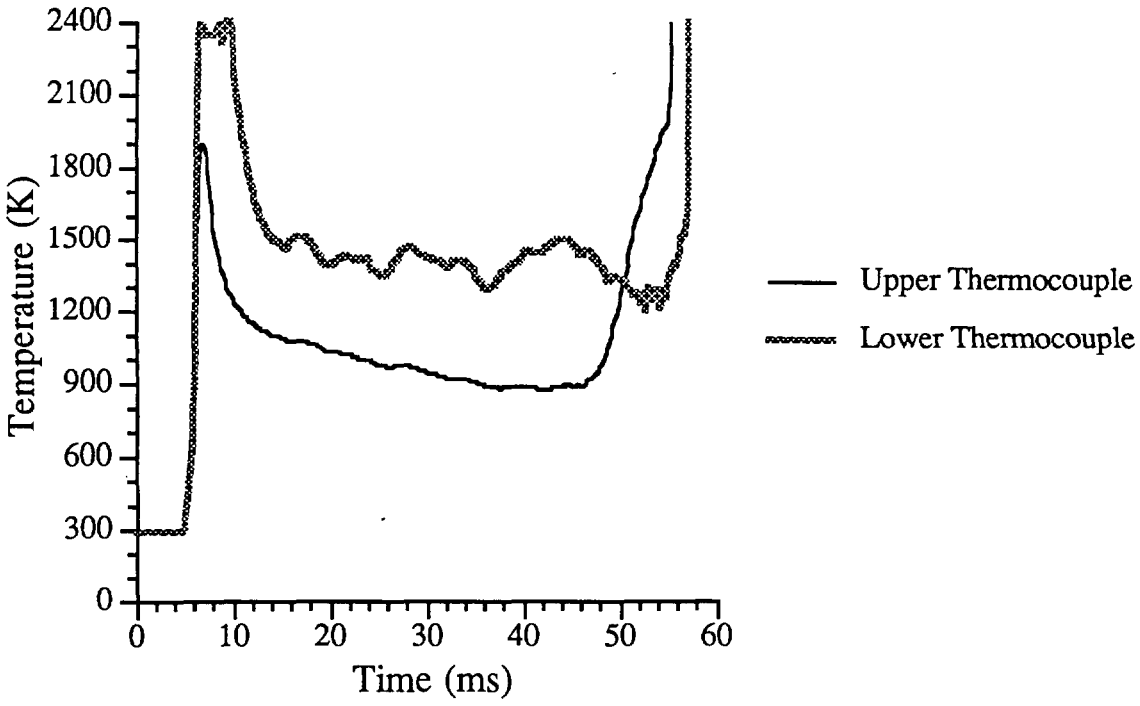

Figure 13. Temperature-history traces of upper and lower thermocouples with M43 propellant.

After the initial exothermal response from the propellant, the temperature decreased to about 1200 K and then slowly declined to about 900 K. During this time, about 40 ms, a "hang-fire" ignition occurred. In other words, the propellant received the ignition stimulus and appeared not to react during a long induction period. At the end of this period, combustion rapidly took place throughout the propellant bed and in less than 10 ms the thermocouples reported thermal runaway. During the runaway, the chamber pressure also rapidly increased until sufficient pressure was generated to activate the rupture disk and eject the burning propellant into the waiting water bath for quenching of the remaining propellant.

4. SUMMARY

Platinum versus 10% Rh/platinum fine-wire thermocouple were used to obtain gas-phase temperatures within a propellant bed. Probe mounts that provided sufficient physical support for the fine-wire thermocouples and minimally perturbed the flow environment were designed and evaluated. Different thermocouple wire diameters also were evaluated for their response (lag) times. Two thermocouples of differing diameter were placed in the same probe mount so that the same thermal environment was sampled by both. This configuration was evaluated for systemic errors. No apparent biasing of the measurement was noted. The largest diameter thermocouple (3 mil or 76 μm) exhibited a response time too great for determining temperatures during the ignition phase of a propellant bed. The smallest diameter (1 mil or 25 μm) exhibited the shortest response time and would be the thermocouple of choice for this experiment; however, it was not used in the current experiments due to difficulties in probe fabrication and consideration of the wire strength. The 2-mil (51 μm) wire was judged adequate except possibly during the very early heating phase in which the temperature rises very rapidly (in this case, an event that approximated a step function).

Theoretically (Equations 8-12), each succeeding smaller diameter will show a deviation from the larger diameter during times of rapid gas movement because the convective heat transfer coefficient varies with the inverse of approximately the square root of the diameter. As the gas velocity diminishes and heat transfer is controlled primarily by conduction, the indicated temperatures of both large and small thermocouples become equal. Implicit in Equation 12 are two extensive properties of the thermocouple junction that affect the lag time. Namely, the product of the volumetric heat capacity and the junction diameter reflects the ratio of the mass of the junction to its surface area. As the mass (diameter) of the junction increases, so does the lag time. However, as the surface area that is presented for heat transfer increases, the lag time decreases. Therefore, the ideal junction should consist of the least amount of mass but should present a maximum surface area to the gas flow. Both these conditions make a thermocouple junction that is weak and would not survive a rapid gas flow. Thus, a bargain is struck between extreme rapidity and surviving the event long enough to provide useful data.

The reporting difference due to convection during rapid gas flow was demonstrated by the indicated temperatures reported by both large and small thermocouples [reporting pairs of 3- and 2-mil diameter (76 and 51 μm) and of 2- and 1-mil (51 and 25 μm) diameter wires] in the double mount. At long times when the convective flow had diminished to essentially zero, the indicated temperatures by each member of the reporting pair asymptotically approached the same value.

Two sources of possible error in the thermocouple measurement (catalytic heating and radiative heat loss) were investigated and the magnitude of each error determined. Gas-phase concentrations of radicals were obtained via a NASA-Lewis equilibrium code and the maximum temperature due to catalytic reactions on the thermocouple surface determined. Temperature error due to catalytic effects was estimated to be less than 1 K and was subsequently ignored. Radiative corrections to the temperatures were mainly dependent on the thermocouple material and emissivity. These values were obtained from the thermocouple manufacturer. The experimental parameter related to the experiment was the gas mixture thermal conductivity. This property was estimated from engineering expressions that were corrected for composition by the NASA-Lewis equilibrium simulation code. The magnitude of the correction for the thermocouples was computed to be approximately 30 K in the region of peak temperature for each of the three thermocouples.

Tests with inert propellant beds indicated a peak gas temperature in the region of 1200 K at a pressure of approximately 3 MPa in the flow chamber. These conditions are thought to be representative of those present in some ignition systems. Preliminary tests also indicate that ignition characteristics are highly dependent upon the physical condition of the propellant bed and the manner of introduction of the hot gases into the bed. These results and others (see Kooker, Howard, and Chang 1993) show promise of tailoring the ignition stimulus so that different parameters of the hang-fire condition can be investigated.

5. REFERENCES

Alberty, R. A. and F. Daniels. Physical Chemistry, 5th edition, John Wiley & Sons, New York, 1979, Chapter 14.

Baker, H. D., E. A. Ryder, and N. H. Baker. Temperature Measurement in Engineering, vol. II, Omega Press, Stamford, Chapter 6, 1975.

Brosseau, T. L., I. C. Stobie, J. R. Ward, and R. W. Geene. "120 mm Gun Heat Input Measurements." ARBRL-TR-02413, U. S. Army Ballistic Research Laboratory, July 1982.

Brosseau T. L. and J. R. Ward. "Reduction of Heat Transfer in 105 mm Tank Gun by Wear-Reducing Additives." BRL-MR-2698, U. S. Army Ballistic Research Laboratory, November 1976.

Brosseau T. L. and J. R. Ward. "Measurement of the Heat Input into the 105 mm M68 Tank Cannon Firing Rounds Equipped with Wear-Reducing Additives." BRL-TR-02056, U. S. Army Ballistic Research Laboratory, April 1978.

Chang, L.-M., R. W. Deas, and J. Grosh. "Ignition Studies of Two-Piece Cartridges for an Advanced Tank Cannon System (ATACS)." BRL-TR-3249, U. S. Army Ballistic Research Laboratory, August 1991.

Chang, L.-M. and J. J. Rocchio. "Simulator Diagnostics of the Early Phase Ignition Phenomena in a 105-mm Tank Gun Chamber." BRL-TR-2890, U. S. Army Ballistic Research Laboratory, March 1988.

Gordon, S. and B. J. McBride. "Computer Program for Calculation of Complex Chemical Equilibrium Compositions, Rocket Performance, Incident and Reflected Shocks, and Chapman-Jouguet Detonations." NASA SP-273, NASA Lewis Research Center, March 1976.

Hayhurst, A. N. and D. B. Kittelson. "Heat and Mass Transfer Considerations in the Use of Electrically Heated Thermocouples of Iridium versus an Iridium/Rhodium Alloy in Atmospheric Pressure Flames." Combustion and Flame, vol. 28, p. 301, 1977.

Horst, A. W. "Multiphase Flow Analysis of the Ballistic Performance of an Anomalous LOVA Propellant Mix." 20th JANNAF Combustion Meeting, CPIA Publication 383, vol. I, p. 557, October 1983.

Horst, A. W. "Breechblow Phenomenology Revised." BRL-TR-2707, U. S. Army Ballistic Research Laboratory, January 1986.

Kent, J. H. "A Noncatalytic Coating for Platinum-Rhodium Thermocouples." Combustion and Flame, vol. 14, p. 279, 1970.

Klingenberg, G. and H. Mach. "Experimental Study of Non-Steady Phenomena Associated with the Combustion of Solid Gun Propellants." Proceedings of the 16th Symposium (International) on Combustion, Cambridge, Massachusetts, August 15-21, 1976.

Knudsen, J. G., K. J. Bell, A. D. Holt, H. C. Hottel, A. D. Sarofim, F. C. Standiford, D. Stuhlbarg, and V. W. Uhl. "Heat Transmission." Chemical Engineer's Handbook, 5th ed.; Perry, R. H.; Chilton, C. H. Eds., McGraw-Hill, New York, Section 10, 1973.

Kooker, D. E., L.-M. Chang, and S. L. Howard. "Flamespreading in Granular Solid Propellant: Design of an Experiment." ARL-MR-80, U. S. Army Ballistic Research Laboratory, June 1993.

Kooker, D. E., S. L. Howard, and L.-M. Chang. "Flamespreading in Granular Solid Propellant: Initial Results." 30th JANNAF Combustion Meeting, CPIA Publication 606, vol. I, November 1993.

Kracek, F. C. and W. J. Benedict. "Temperature of Propellant Gases." National Defense Research Committee, Armour and Ordnance Report No. A-201, July 1943.

Kracek, F. C. and W. J. Benedict. "An Experimental Study of Powder Gas Radiation and Temperature." National Defense Research Committee, Armour and Ordnance Report No. A-252, February 1944.

Liley, P. E. and W. R. Gambill. Chemical Engineer's Handbook, 5th ed.; Perry, R. H.; Chilton, C. H. Eds., McGraw-Hill, New York, 1973, Section 3.

May, I. W., and A. W. Horst. "Charge Design Considerations and Effect on Pressure Waves in Gun." ARBRL-TR-0277, U. S. Army Ballistic Research Laboratory, December 1978.

Miller, M. S. "Modeling of Kinetics and Combustion of Energetic Materials." ARO-URI Meeting on Fast Reaction Kinetics and Modeling of Energetic Material Combustion, The Pennsylvania State University, State College, PA, August 1992.

McClure, D. R. Measurement of Gas Temperature and Convective Heat Flux in a Reacting Granular Propellant Bed, Ph.D. Dissertation Thesis, Pennsylvania State University, Pennsylvania, 1984.

Penzias, G. J. "Temperature Measurement and Gas Analysis in Flames and Plasmas Using Spectroscopic Methods." Combustion Technology: Some Modern Developments, Palmer, E. and Y. Beer, Eds., Academic Press, New York, 1974.

Peterson, R. C. PhD Thesis, Purdue University, 1981.

Schlichting, H. Boundary Layer Theory, McGraw-Hill, New York, 1960a, p. 25.

Schlichting, H. Boundary Layer Theory, McGraw-Hill, New York, 1960b, p. 537.

Stobie, I. C., T. L. Brosseau, and R. P. Kaste. "Heat Measurements in 105 mm Tank Gun with M735 Rounds." ARBRL-TR-02265, U. S. Army Ballistic Research Laboratory, September 1980.

Tourin, R. H. Spectroscopic Gas Temperature Measurement, Elsevier Publishing Co., Amsterdam, 1966.

Vanderhoff, J. A., W. R. Anderson, and A. J. Kotlar. "Dark Zone Modeling of Solid Propellant Flames." 29th JANNAF Combustion Meeting, CPIA Publication 593, vol. II, p. 225, October 1992.

Weast, R. C. and M. J. Astle, Eds., CRC Handbook of Chemistry and Physics, CRC Press, Inc., Boca Raton, 1980.

No. of Copies	Organization
2	Administrator Defense Technical Info Center ATTN: DTIC-DDA Cameron Station Alexandria, VA 22304-6145
1	Commander U.S. Army Materiel Command ATTN: AMCAM 5001 Eisenhower Ave. Alexandria, VA 22333-0001
1	Director U.S. Army Research Laboratory ATTN: AMSRL-OP-CI-AD, Tech Publishing 2800 Powder Mill Rd. Adelphi, MD 20783-1145
1	Director U.S. Army Research Laboratory ATTN: AMSRL-OP-CI-AD, Records Management 2800 Powder Mill Rd. Adelphi, MD 20783-1145
2	Commander U.S. Army Armament Research, Development, and Engineering Center ATTN: SMCAR-TDC Picatinny Arsenal, NJ 07806-5000
1	Director Benet Weapons Laboratory U.S. Army Armament Research, Development, and Engineering Center ATTN: SMCAR-CCB-TL Watervliet, NY 12189-4050
1	Director U.S. Army Advanced Systems Research and Analysis Office (ATCOM) ATTN: AMSAT-R-NR, M/S 219-1 Ames Research Center Moffett Field, CA 94035-1000

No. of Copies	Organization
1	Commander U.S. Army Missile Command ATTN: AMSMI-RD-CS-R (DOC) Redstone Arsenal, AL 35898-5010
1	Commander U.S. Army Tank-Automotive Command ATTN: AMSTA-JSK (Armor Eng. Br.) Warren, MI 48397-5000
1	Director U.S. Army TRADOC Analysis Command ATTN: ATRC-WSR White Sands Missile Range, NM 88002-5502
(Class. only) 1	Commandant U.S. Army Infantry School ATTN: ATSH-CD (Security Mgr.) Fort Benning, GA 31905-5660
(Unclass. only) 1	Commandant U.S. Army Infantry School ATTN: ATSH-WCB-O Fort Benning, GA 31905-5000

Aberdeen Proving Ground

2	Dir, USAMSAA ATTN: AMXSY-D AMXSY-MP, H. Cohen
1	Cdr, USATECOM ATTN: AMSTE-TC
1	Dir, USAERDEC ATTN: SCBRD-RT
1	Cdr, USACBDCOM ATTN: AMSCB-CII
1	Dir, USARL ATTN: AMSRL-SL-I
5	Dir, USARL ATTN: AMSRL-OP-AP-L

No. of Copies	Organization
2	HQDA ATTN: SARD-TR/Ms. K. Kominos SARD-TR/Dr. R. Chait Washington, DC 20310-0103
2	HQDA ATTN: SARD-TT/Dr. F. Milton SARD-TT/Mr. J. Appel Washington, DC 20310-0103
1	Chairman DOD Explosives Safety Board Room 856-C Hoffman Bldg. 1 2461 Eisenhower Avenue Alexandria, VA 22331-0600
1	Headquarters U.S. Army Materiel Command ATTN: AMCICP-AD, M. Fisette 5001 Eisenhower Ave. Alexandria, VA 22333-0001
1	U.S. Army Ballistic Missile Defense Systems Command Advanced Technology Center P.O. Box 1500 Huntsville, AL 35807-3801
1	Department of the Army Office of the Product Manager 155mm Howitzer, M109A6, Paladin ATTN: SFAE-AR-HIP-IP, Mr. R. De Kleine Picatinny Arsenal, NJ 07806-5000
3	Project Manager Advanced Field Artillery System ATTN: SFAE-ASM-AF-E, LTC A. Ellis T. Kuriata J. Shields Picatinny Arsenal, NJ 07801-5000
1	Project Manager Advanced Field Artillery System ATTN: SFAE-ASM-AF-Q, W. Warren Picatinny Arsenal, NJ 07801-5000

No. of Copies	Organization
1	Commander Production Base Modernization Agency U.S. Army Armament Research, Development, and Engineering Center ATTN: AMSMC-PBM, A. Siklosi Picatinny Arsenal, NJ 07806-5000
1	Commander Production Base Modernization Agency U.S. Army Armament Research, Development, and Engineering Center ATTN: AMSMC-PBM-E, L. Laibson Picatinny Arsenal, NJ 07806-5000
1	PEO-Armaments Project Manager Tank Main Armament System ATTN: AMCPM-TMA Picatinny Arsenal, NJ 07806-5000
1	PEO-Armaments Project Manager Tank Main Armament System ATTN: AMCPM-TMA-105 Picatinny Arsenal, NJ 07806-5000
1	PEO-Armaments Project Manager Tank Main Armament System ATTN: AMCPM-TMA-120 Picatinny Arsenal, NJ 07806-5000
1	PEO-Armaments Project Manager Tank Main Armament System ATTN: AMCPM-TMA-AS, H. Yuen Picatinny Arsenal, NJ 07806-5000
2	Commander U.S. Army Armament Research, Development, and Engineering Center ATTN: SMCAR-CCH-V, C. Mandala E. Fennell Picatinny Arsenal, NJ 07806-5000
1	Commander U.S. Army Armament Research, Development, and Engineering Center ATTN: SMCAR-CCH-T, L. Rosendorf Picatinny Arsenal, NJ 07806-5000

No. of Copies	Organization
1	Commander U.S. Army Armament Research, Development, and Engineering Center ATTN: SMCAR-CCS Picatinny Arsenal, NJ 07806-5000
1	Commander U.S. Army Armament Research, Development, and Engineering Center ATTN: SMCAR-AEE, J. Lannon Picatinny Arsenal, NJ 07806-5000
11	Commander U.S. Army Armament Research, Development, and Engineering Center ATTN: SMCAR-AEE-B, A. Beardell D. Downs S. Einstein S. Westley S. Bernstein J. Rutkowski B. Brodman P. O'Reilly R. Cirincione P. Hui J. O'Reilly Picatinny Arsenal, NJ 07806-5000
5	Commander U.S. Army Armament Research, Development, and Engineering Center ATTN: SMCAR-AEE-WW, M. Mezger J. Pinto D. Wiegand P. Lu C. Hu Picatinny Arsenal, NJ 07806-5000
1	Commander U.S. Army Armament Research, Development, and Engineering Center ATTN: SMCAR-AES, S. Kaplowitz Picatinny Arsenal, NJ 07806-5000
1	Commander U.S. Army Armament Research, Development and Engineering Center ATTN: SMCAR-HFM, E. Barrieres Picatinny Arsenal, NJ 07806-5000
1	Commander U.S. Army Armament Research, Development and Engineering Center ATTN: SMCAR-FSA-T, M. Salsbury Picatinny Arsenal, NJ 07806-5000
1	Commander U.S. Army Armament Research, Development and Engineering Center ATTN: SMCAR-FSA-F, LTC R. Riddle Picatinny Arsenal, NJ 07806-5000
1	Commander U.S. Army Armament Research, Development and Engineering Center ATTN: SMCAR-FSC, G. Ferdinand Picatinny Arsenal, NJ 07806-5000
1	Commander U.S. Army Armament Research, Development and Engineering Center ATTN: SMCAR-FS, T. Gora Picatinny Arsenal, NJ 07806-5000
1	Commander U.S. Army Armament Research, Development and Engineering Center ATTN: SMCAR-FS-DH, J. Feneck Picatinny Arsenal, NJ 07806-5000
3	Commander U.S. Army Armament Research, Development and Engineering Center ATTN: SMCAR-FSS-A, R. Kopmann B. Machek L. Pinder Picatinny Arsenal, NJ 07806-5000
1	Commander U.S. Army Armament Research, Development and Engineering Center ATTN: SMCAR-FSN-N, K. Chung Picatinny Arsenal, NJ 07806-5000
4	Director Benet Weapons Laboratories ATTN: SMCAR-CCB-RA, G.P. O'Hara G.A. Pflegl SMCAR-CCB-RT, S. Sopok SMCAR-CCB-S, F. Heiser Watervliet, NY 12189-4050

No. of Copies	Organization
2	Commander U.S. Army Research Office ATTN: Technical Library D. Mann P.O. Box 12211 Research Triangle Park, NC 27709-2211
1	Commander, USACECOM R&D Technical Library ATTN: ASQNC-ELC-IS-L-R, Myer Center Fort Monmouth, NJ 07703-5301
1	Director U.S. Army Research Laboratory ATTN: AMSRL-D 2800 Powder Mill Rd. Adelphi, MD 20783-1145
1	Commandant U.S. Army Aviation School ATTN: Aviation Agency Fort Rucker, AL 36360
1	Program Manager U.S. Tank-Automotive Command ATTN: AMCPM-ABMS, T. Dean Warren, MI 48092-2498
1	Project Manager U.S. Tank-Automotive Command Fighting Vehicle Systems ATTN: SFAE-ASM-BV Warren, MI 48397-5000
1	Project Manager, Abrams Tank System ATTN: SFAE-ASM-AB Warren, MI 48397-5000
1	Director HQ, TRAC RPD ATTN: ATCD-MA Fort Monroe, VA 23651-5143
1	Commander U.S. Army Belvoir Research and Development Center ATTN: STRBE-WC Fort Belvoir, VA 22060-5006

No. of Copies	Organization
1	Director U.S. Army TRAC-Ft. Lee ATTN: ATRC-L, Mr. Cameron Fort Lee, VA 23801-6140
1	Commandant U.S. Army Command and General Staff College Fort Leavenworth, KS 66027
1	Commandant U.S. Army Special Warfare School ATTN: Rev and Trng Lit Div Fort Bragg, NC 28307
1	Commander Radford Army Ammunition Plant ATTN: SMCAR-QA/HI LIB Radford, VA 24141-0298
1	Commander U.S. Army Foreign Science and Technology Center ATTN: AMXST-MC-3 220 Seventh Street, NE Charlottesville, VA 22901-5396
2	Commandant U.S. Army Field Artillery Center and School ATTN: ATSF-CD, COL T. Stricklin ATSF-CN, P. Gross Ft. Sill, OK 73503-5600
1	Commandant U.S. Army Armor School ATTN: ATZK-CD-MS, M. Falkovitch Armor Agency Fort Knox, KY 40121-5215
1	U.S. Army European Research Office ATTN: Dr. Roy E. Richenbach Box 65 FPO New York 09510-1500
2	Commander Naval Sea Systems Command ATTN: SEA 62R SEA 64 Washington, DC 20362-5101

No. of Copies	Organization
1	Commander Naval Air Systems Command ATTN: AIR-954-Tech Library Washington, DC 20360
4	Commander Naval Research Laboratory ATTN: Technical Library Code 4410, K. Kailasanate J. Boris E. Oran Washington, DC 20375-5000
1	Office of Naval Research ATTN: Code 473, R.S. Miller 800 N. Quincy Street Arlington, VA 22217-9999
1	Office of Naval Technology ATTN: ONT-213, D. Siegel 800 N. Quincy St. Arlington, VA 22217-5000
2	Commander Naval Surface Warfare Center ATTN: Code 730 Code R-13, R. Bernecker Silver Spring, MD 20903-5000
7	Commander Naval Surface Warfare Center ATTN: T.C. Smith K. Rice S. Mitchell S. Peters J. Consaga C. Gotzmer Technical Library Indian Head, MD 20640-5000
4	Commander Naval Surface Warfare Center ATTN: Code G30, Guns & Munitions Div Code G32, Guns Systems Div Code G33, T. Doran Code E23 Technical Library Dahlgren, VA 22448-5000

No. of Copies	Organization
5	Commander Naval Air Warfare Center ATTN: Code 388, C.F. Price T. Boggs Code 3895, T. Parr R. Derr Information Science Division China Lake, CA 93555-6001
1	Commanding Officer Naval Underwater Systems Center ATTN: Code 5B331, Technical Library Newport, RI 02840
1	AFOSR/NA ATTN: J. Tishkoff Bolling AFB, D.C. 20332-6448
1	OLAC PL/TSTL ATTN: D. Shiplett Edwards AFB, CA 93523-5000
3	AL/LSCF ATTN: J. Levine L. Quinn T. Edwards Edwards AFB, CA 93523-5000
1	WL/MNAA ATTN: B. Simpson Eglin AFB, FL 32542-5434
1	WL/MNME Energetic Materials Branch 2306 Perimeter Rd. STE 9 Eglin AFB, FL 32542-5910
1	WL/MNSH ATTN: R. Drabczuk Eglin AFB, FL 32542-5434
2	NASA Langley Research Center ATTN: M.S. 408, W. Scallion D. Witcofski Hampton, VA 23605

No. of Copies	Organization
1	Central Intelligence Agency Office of the Central References Dissemination Branch Room GE-47, HQS Washington, DC 20502
1	Central Intelligence Agency ATTN: J. Backofen NHB, Room 5N01 Washington, DC 20505
1	SDIO/TNI ATTN: L.H. Caveny Pentagon Washington, DC 20301-7100
1	SDIO/DA ATTN: E. Gerry Pentagon Washington, DC 21301-7100
2	HQ DNA ATTN: D. Lewis A. Fahey 6801 Telegraph Rd. Alexandria, VA 22310-3398
1	Director Sandia National Laboratories Energetic Materials & Fluid Mechanics Department, 1512 ATTN: M. Baer P.O. Box 5800 Albuquerque, NM 87185
1	Director Sandia National Laboratories Combustion Research Facility ATTN: R. Carling Livermore, CA 94551-0469
1	Director Sandia National Laboratories ATTN: 8741, G. A. Beneditti P.O. Box 969 Livermore, CA 94551-0969

No. of Copies	Organization
2	Director Lawrence Livermore National Laboratory ATTN: L-355, A. Buckingham M. Finger P.O. Box 808 Livermore, CA 94550-0622
2	Director Los Alamos Scientific Lab ATTN: T3/D. Butler M. Division/B. Craig P.O. Box 1663 Los Alamos, NM 87544
2	Battelle ATTN: TACTEC Library, J.N. Huggins V. Levin 505 King Avenue Columbus, OH 43201-2693
1	Battelle PNL ATTN: Mr. Mark Garnich P.O. Box 999 Richland, WA 99352
1	Institute of Gas Technology ATTN: D. Gidaspow 3424 S. State Street Chicago, IL 60616-3896
1	Institute for Advanced Technology ATTN: T.M. Krehne The University of Texas of Austin 4030-2 W. Braker Lane Austin, TX 78759-5329
2	CPIA - JHU ATTN: H. J. Hoffman T. Christian 10630 Little Patuxent Parkway Suite 202 Columbia, MD 21044-3200
1	AFELM, The Rand Corporation ATTN: Library D 1700 Main Street Santa Monica, CA 90401-3297

No. of Copies	Organization
1	Brigham Young University Department of Chemical Engineering ATTN: M. Beckstead Provo, UT 84601
1	Jet Propulsion Laboratory California Institute of Technology ATTN: L.D. Strand, MS 125/224 4800 Oak Grove Drive Pasadena, CA 91109
1	California Institute of Technology 204 Karman Lab Main Stop 301-46 ATTN: F.E.C. Culick 1201 E. California Street Pasadena, CA 91109
3	Georgia Institute of Technology School of Aerospace Engineering ATTN: B.T. Zim E. Price W.C. Strahle Atlanta, GA 30332
2	University of Illinois Department of Mechanical/Industry Engineering ATTN: H. Krier R. Beddini 144 MEB; 1206 N. Green St. Urbana, IL 61801-2978
1	University of Massachusetts Department of Mechanical Engineering ATTN: K. Jakus Amherst, MA 01002-0014
1	University of Minnesota Department of Mechanical Engineering ATTN: E. Fletcher Minneapolis, MN 55414-3368
3	Pennsylvania State University Department of Mechanical Engineering ATTN: V. Yang K. Kuo C. Merkle University Park, PA 16802-7501
1	Rensselaer Polytechnic Institute Department of Mathematics Troy, NY 12181
1	Stevens Institute of Technology Davidson Laboratory ATTN: R. McAlevy III Castle Point Station Hoboken, NJ 07030-5907
1	Rutgers University Department of Mechanical and Aerospace Engineering ATTN: S. Temkin University Heights Campus New Brunswick, NJ 08903
1	University of Utah Department of Chemical Engineering ATTN: A. Baer Salt Lake City, UT 84112-1194
1	Washington State University Department of Mechanical Engineering ATTN: C.T. Crowe Pullman, WA 99163-5201
1	Arrow Technology Associates, Inc. ATTN: W. Hathaway P.O. Box 4218 South Burlington, VT 05401-0042
3	AAI Corporation ATTN: J. Hebert J. Frankle D. Cleveland P.O. Box 126 Hunt Valley, MD 21030-0126
8	Alliant Techsystems, Inc. ATTN: R.E. Tompkins J. Kennedy J. Bode C. Candland L. Osgood R. Buretta R. Becker M. Swenson 600 Second St. NE Hopkins, MN 55343

No. of Copies	Organization
1	General Applied Sciences Lab ATTN: J. Erdos 77 Raynor Ave. Ronkonkama, NY 11779-6649
1	General Electric Company Tactical System Department ATTN: J. Mandzy 100 Plastics Ave. Pittsfield, MA 01201-3698
1	IITRI ATTN: M.J. Klein 10 W. 35th Street Chicago, IL 60616-3799
4	Hercules, Inc. Radford Army Ammunition Plant ATTN: L. Gizzi D.A. Worrell W.J. Worrell C. Chandler Radford, VA 24141-0299
2	Hercules, Inc. Allegheny Ballistics Laboratory ATTN: William B. Walkup Thomas F. Farabaugh P.O. Box 210 Rocket Center, WV 26726
1	Hercules, Inc. Aerospace ATTN: R. Cartwright 100 Howard Blvd. Kenville, NJ 07847
1	Hercules, Inc. Hercules Plaza ATTN: B.M. Riggleman Wilmington, DE 19894
1	Martin Marietta Armament Systems ATTN: Jim Talley Room 1309 Lakeside Avenue Burlington, VT 05401
1	MBR Research Inc. ATTN: Dr. Moshe Ben-Reuven 601 Ewing St., Suite C-22 Princeton, NJ 08540

No. of Copies	Organization
1	Olin Corporation Badger Army Ammunition Plant ATTN: F.E. Wolf Baraboo, WI 53913
3	Olin Ordnance ATTN: E.J. Kirschke A.F. Gonzalez D.W. Worthington P.O. Box 222 St. Marks, FL 32355-0222
1	Olin Ordnance ATTN: H.A. McElroy 10101 9th Street, North St. Petersburg, FL 33716
1	Paul Gough Associates, Inc. ATTN: P.S. Gough 1048 South St. Portsmouth, NH 03801-5423
1	Physics International Library ATTN: H. Wayne Wampler P.O. Box 5010 San Leandro, CA 94577-0599
2	Princeton Combustion Research Laboratories, Inc. ATTN: N. Mer N.A. Messina Princeton Corporate Plaza 11 Deerpark Dr., Bldg IV, Suite 119 Monmouth Junction, NJ 08852
3	Rockwell International Rocketdyne Division ATTN: BA08, J. Flanagan J. Gray R.B. Edelman 6633 Canoga Avenue Canoga Park, CA 91303-2703
2	Rockwell International Science Center ATTN: Dr. S. Chakravarthy Dr. S. Palaniswamy 1049 Camino Dos Rios P.O. Box 1085 Thousand Oaks, CA 91360

No. of Copies	Organization
1	Science Applications International Corp. ATTN: M. Palmer 2109 Air Park Rd. Albuquerque, NM 87106
1	Southwest Research Institute ATTN: J.P. Riegel 6220 Culebra Road P.O. Drawer 28510 San Antonio, TX 78228-0510
1	Sverdrup Technology, Inc. ATTN: Dr. John Deur 2001 Aerospace Parkway Brook Park, OH 44142
3	Thiokol Corporation Elkton Division ATTN: R. Willer R. Biddle Tech Library P.O. Box 241 Elkton, MD 21921-0241
1	Veritay Technology, Inc. ATTN: E. Fisher 4845 Millersport Hwy. East Amherst, NY 14501-0305
1	Universal Propulsion Company ATTN: H.J. McSpadden 25401 North Central Ave. Phoenix, AZ 85027-7837
1	SRI International Propulsion Sciences Division ATTN: Tech Library 333 Ravenwood Avenue Menlo Park, CA 94025-3493
	Aberdeen Proving Ground
1	Cdr, USACSTA ATTN: STECS-LI/R. Hendricksen

INTENTIONALLY LEFT BLANK.

USER EVALUATION SHEET/CHANGE OF ADDRESS

This Laboratory undertakes a continuing effort to improve the quality of the reports it publishes. Your comments/answers to the items/questions below will aid us in our efforts.

1. ARL Report Number ARL-MR-146 Date of Report August 1994

2. Date Report Received _____

3. Does this report satisfy a need? (Comment on purpose, related project, or other area of interest for which the report will be used.) _____

4. Specifically, how is the report being used? (Information source, design data, procedure, source of ideas, etc.) _____

5. Has the information in this report led to any quantitative savings as far as man-hours or dollars saved, operating costs avoided, or efficiencies achieved, etc? If so, please elaborate. _____

6. General Comments. What do you think should be changed to improve future reports? (Indicate changes to organization, technical content, format, etc.) _____

CURRENT ADDRESS

_____
Organization

_____
Name

_____
Street or P.O. Box No.

_____
City, State, Zip Code

7. If indicating a Change of Address or Address Correction, please provide the Current or Correct address above and the Old or Incorrect address below.

OLD ADDRESS

_____
Organization

_____
Name

_____
Street or P.O. Box No.

_____
City, State, Zip Code

(Remove this sheet, fold as indicated, tape closed, and mail.)
(DO NOT STAPLE)

DEPARTMENT OF THE ARMY

OFFICIAL BUSINESS

NO POSTAGE
NECESSARY
IF MAILED
IN THE
UNITED STATES

BUSINESS REPLY MAIL
FIRST CLASS PERMIT NO 0001, APG, MD

Postage will be paid by addressee

Director
U.S. Army Research Laboratory
ATTN: AMSRL-OP-AP-L
Aberdeen Proving Ground, MD 21005-5066